© 2022. Published by The Company of Biologists Ltd | Development (2022) 149, dev200131. doi:10.1242/dev.200131

RESEARCH ARTICLE

FOXO1 represses sprouty 2 and sprouty 4 expression to promote arterial specification and vascular remodeling in the mouse yolk sac

Nanbing Li-Villarreal*, Rebecca Lee Yean Wong*, Monica D. Garcia*, Ryan S. Udan, Ross A. Poché, Tara L. Rasmussen, Alexander M. Rhyner, Joshua D. Wythe and Mary E. Dickinson‡

ABSTRACT

Establishing a functional circulatory system is required for post-implantation development during murine embryogenesis. Previous studies in loss-of-function mouse models showed that FOXO1, a Forkhead family transcription factor, is required for yolk sac (YS) vascular remodeling and survival beyond embryonic day (E) 11. Here, we demonstrate that at E8.25, loss of *Foxo1* in *Tie2-cre* expressing cells resulted in increased sprouty 2 (*Spry2*) and *Spry4* expression, reduced arterial gene expression and reduced *Kdr* (also known as *Vegfr2* and *Flk1*) transcripts without affecting overall endothelial cell identity, survival or proliferation. Using a *Dll4-BAC-nlacZ* reporter line, we found that one of the earliest expressed arterial genes, delta like 4, is significantly reduced in *Foxo1* mutant YS without being substantially affected in the embryo proper. We show that FOXO1 binds directly to previously identified *Spry2* gene regulatory elements (GREs) and newly identified, evolutionarily conserved *Spry4* GREs to repress their expression. Furthermore, overexpression of *Spry4* in transient transgenic embryos largely recapitulates the reduced expression of arterial genes seen in conditional *Foxo1* mutants. Together, these data reveal a novel role for FOXO1 as a key transcriptional repressor regulating both pre-flow arterial specification and subsequent vessel remodeling within the murine YS.

KEY WORDS: Arterial specification, Dll4, Foxo1, Sprouty

INTRODUCTION

During early development, the mammalian embryo requires a functional circulatory system to distribute oxygen, nutrients and hormones. The mammalian heart is the first organ to form and function within this early embryo, along with the first arteries and veins that arise *de novo* via vasculogenesis (Fish and Wythe, 2015; Risau, 1994; Risau and Flamme, 1995; Chong et al., 2011). Primitive erythrocytes form in the blood islands of the extra-embryonic yolk sac (YS), and are drawn into circulation as the heart begins to beat around embryonic day (E) 8 in the mouse embryo (Lucitti et al., 2007; Palis, 2014; Ji et al., 2003). A complete circulatory loop between the embryo and the extra-embryonic YS is evident shortly after the onset of cardiac contractions, with blood flowing through the dorsal aorta to the vitelline (omphalomesenteric) artery (VA), through the YS capillary plexus, and back through the vitelline (omphalomesenteric) vein (VV) to the sinus venosus of the heart. Circulation through the YS is the main circulatory loop until the chorio-allantoic placenta connections develop later, around E9.

A key finding several years ago showed that arterial-venous (AV) identity is established before the onset of blood flow in the early mouse embryo (Herzog et al., 2005; Chong et al., 2011; Aitsebaomo et al., 2008; Wang et al., 1998; Adams et al., 1999). Others have since shown that some aspects of AV identity are plastic, as they can be influenced by changes in blood flow and hemodynamics (le Noble et al., 2004, 2005; Wragg et al., 2014). Extensive work in zebrafish showed that AV specification depends on differential responses to VEGF signaling through the tyrosine kinase receptor KDR (also known as VEGFR2 and FLK1), high levels of which activate the MEK/ERK kinase cascade in arterial cells and PI3 K/AKT signaling in venous cells (Fish and Wythe, 2015; Covassin et al., 2006; Weinstein and Lawson, 2002). In the arterial endothelium, VEGFR2 signaling stimulates the Notch pathway, which in turn promotes an arterial identity while simultaneously repressing a venous fate (Weinstein and Lawson, 2002; Krebs et al., 2010, 2000; Lawson et al., 2001, 2002; Liu et al., 2003; Shutter et al., 2000; Swift and Weinstein, 2009; Siekmann and Lawson, 2007; Duarte et al., 2004; Lobov et al., 2007). VEGF upregulates expression of delta-like 4 (*Dll4*), which encodes a ligand for the Notch family of transmembrane receptors. *Dll4* is the earliest Notch ligand expressed in arterial cells in the early mouse embryo (Shutter et al., 2000; Mailhos et al., 2001; Wythe et al., 2013; Cleaver and Krieg, 1998; Chong et al., 2011), and is essential for AV patterning (Krebs et al., 2000; Gale et al., 2004; Duarte et al., 2004). Expression of *Dll4* depends on the activation of ETS transcription factors, which are downstream of VEGF signaling (Wythe et al., 2013; Fish et al., 2017), and *Dll4* mRNA expression can be increased by shear stress (Masumura et al., 2009; Obi et al., 2009). However, the expression of *Dll4* and a few other select arterial markers before, and independently of, the onset of blood flow (Chong et al., 2011; Wang et al., 1998) suggests flow-independent mechanisms regulate arterial specification. VEGFR2 also upregulates expression of the main endothelial cell surface receptor for DLL4, NOTCH1 (Lawson et al., 2002). NOTCH1 itself is activated by blood flow, and the strength of this signal depends on the magnitude of shear stress (Masumura et al., 2009; Mack et al., 2017). NOTCH1 regulates cell junctions and cell cycle arrest, and induces an arterial gene expression program via a connexin 37 (*Gja4*) and *Cdkn1b* (previously known as $p27^{Kip1}$) pathway (Mack et al., 2017; Su et al., 2018; Fang et al., 2017). Crucially, both VEGFR2 and NOTCH1 are thought to act as

Department of Molecular Physiology and Biophysics, Baylor College of Medicine, One Baylor Plaza, Houston, TX 77030, USA.
*These authors contributed equally to this work

‡Author for correspondence (mdickins@bcm.edu)

N.L., 0000-0002-0688-7197; R.L.Y.W., 0000-0002-2031-9292; R.S.U., 0000-0002-3602-5985; T.L.R., 0000-0002-7721-4918; A.M.R., 0000-0002-9116-8751; J.D.W., 0000-0002-3225-2937; M.E.D., 0000-0003-4372-9638

Handling Editor: Liz Robertson
Received 2 September 2021; Accepted 4 March 2022

Development (2022) 149, dev200131. doi:10.1242/dev.200131

mechanosensors, likely linking arterial specification of ECs and hemodynamic feedback via blood flow to re-enforce and solidify their arterial identity (Mack et al., 2017; Tzima et al., 2005; Mack and Iruela-Arispe, 2018; Shay-Salit et al., 2002).

Forces exerted by blood flow play a clear role in AV specification, and also influence vessel morphogenesis and remodeling in the early embryo (Fang et al., 2017; Masumura et al., 2009; le Noble et al., 2004; Chong et al., 2011; Hwa et al., 2017). Hemodynamic force is both necessary and sufficient to remodel the high-resistance mouse YS capillary plexus into a more complex hierarchical network with a large caliber VA and VV, which progressively leads to smaller diameter vessels (Lucitti et al., 2007). Our lab has shown that murine YS vessel remodeling depends on both vessel fusion and EC migration (Udan et al., 2013). Interestingly, live-imaging studies have shown distinct differences in how arterial and venous cells respond to changes in hemodynamic force (Udan et al., 2013; Kondrychyn et al., 2020; Goetz et al., 2014). These data suggest that pathways that control AV identity, which can be regulated by blood flow, may also influence physical responses of ECs to blood flow, such as migration and motility (which facilitate vessel remodeling).

Despite the knowledge gained regarding the mechanisms regulating AV identity and the discovery of mechanosensors that are required for ECs to sense blood flow, a full understanding of these mechanistic pathways has yet to be realized. A recent analysis estimates that ∼6% of genes in the genome (∼1200) may be required during early cardiovascular development (E9.5-E12.5) (Dickinson et al., 2016). One such gene, and the focus of this study, is *Foxo1* (forkhead box protein O1). Forkhead domain class O transcription factors (FOXOs) integrate different cellular signaling pathways to regulate cellular homeostasis (Paik et al., 2007; Huang and Tindall, 2007; Jiramongkol and Lam, 2020). *daf-16/FoxO* was originally identified as a regulator of dauer formation in *C. elegans* (Albert et al., 1981) and was later shown to control longevity by sensing environmental cues such as hormones, nutrient availability, oxidative stress and energy metabolism via signaling through the insulin, AKT/mTor, JNK and AMPK pathways (Sun et al., 2017). Several studies have since established that *Foxo1* is also required for normal embryonic development in mice. Homozygous null *Foxo1* embryos display a primitive YS vasculature, pericardial edema and disorganized embryonic vessels by E9.5, resulting in lethality by E11.5 (Furuyama et al., 2004; Dharaneeswaran et al., 2014; Hosaka et al., 2004; Sengupta et al., 2012; Wilhelm et al., 2016; Ferdous et al., 2011). Further analysis showed that *Tie2-cre*-mediated loss of *Foxo1* in the endothelium, but not the myocardium, phenocopied germline loss of *Foxo1* (Sengupta et al., 2012), demonstrating the requirement for FOXO1 in the embryonic vasculature. Follow-up studies have since found that FOXO1 controls a variety of different processes in endothelial cells (ECs), including, but not limited to EC proliferation and metabolism (Wilhelm et al., 2016), endothelial barrier function (Beard et al., 2020), sprouting angiogenesis (Kim et al., 2019; Fukumoto et al., 2018; Dang et al., 2017), autophagy (Zhang et al., 2019), EC growth (Riddell et al., 2018; Rudnicki et al., 2018) and migration (Niimi et al., 2017). Despite these studies, the exact function that FOXO1 plays in the early vasculature remains elusive. Given that FOXO1 activity can be modulated in response to fluid shear stress (Chlench et al., 2007; Dixit et al., 2008), combined with our studies showing that hemodynamic force is necessary and sufficient for early vascular remodeling (Lucitti et al., 2007; Udan et al., 2013), and the growing evidence for a role for FOXO1 in cell migration and sprouting angiogenesis (Fosbrink et al., 2006; Niimi et al., 2017; Kim et al., 2019), we sought to define the requirement for FOXO1 in the remodeling vasculature of the early embryonic YS.

Herein, we demonstrate a previously unreported role for FOXO1 in regulating AV identity in the murine YS vasculature. From conditional loss-of-function mutants, where *Foxo1* is deleted specifically in *Tie2-cre*-expressing cells (predominantly ECs) (Eklund and Olsen, 2006; Schlaeger et al., 1997; Kisanuki et al., 2001; Chu et al., 2016), we identified a significant downregulation of arterial gene expression in the mouse YS prior to the onset of blood flow. We also detected a significant reduction in *Flk1* (also known as *Vegfr2*) transcripts, but normal expression levels for other pan-endothelial genes, such as *Pecam1*, indicating that the formation of ECs is not disrupted but rather VEGF signaling is affected. Using a recently developed *Dll4* arterial reporter line (Herman et al., 2018), we showed that *Foxo1* is required for *Dll4* expression in the murine YS, but not in the embryo proper. Further analysis showed that FOXO1 represses expression of sprouty (Spry) genes, which encode inhibitors of Raf/MEK/ERK signaling downstream of FGF and VEGF receptor activation. sprouty factors also modulate angiogenesis by negatively regulating small vessel branching, as well as repressing EC migration (Gong et al., 2013; Wietecha et al., 2011; Lee et al., 2001). Although some researchers have shown that FOXO1 positively regulates sprouty gene expression in the liver (Paik et al., 2007), our studies demonstrate that *Foxo1* loss increased sprouty 2 (*Spry2*) and *Spry4* mRNA levels, suggesting that FOXO1 represses *Spry2* and/or *Spry4* in the murine YS. We went on to find that *Spry4* overexpression throughout the YS and embryo profoundly altered arterial gene expression in the YS but, similar to early FOXO1 loss, had an insignificant effect on these transcripts in the embryo proper. Taken together, these data highlight a novel role for FOXO1 in regulating arteriovenous specification in the early YS and reveal a new mechanism whereby FOXO1 represses sprouty gene expression and downstream signaling in the endothelium.

RESULTS

YS vascular remodeling defects in *Foxo1*^{ECKO} embryos are not due to abnormalities in hemodynamic force or allantois defects

To define the role of FOXO1 in ECs within the early embryo, we conditionally ablated *Foxo1* in the endothelium by crossing female *Foxo1*^{flox} mice (Paik et al., 2007) with male *Tie2-Cre* transgenic mice, producing control (*Tie2-Cre*$^{+/+}$;*FoxO*$^{+/flox}$) and CKO (*Tie2-Cre*$^{+/tg}$;*Foxo1*$^{flox/flox}$, hereafter referred to as *Foxo1*^{ECKO}) embryos, in which Cre recombinase is expressed in endothelial and in hematopoietic cells and progenitors, starting at E7.5 (Kisanuki et al., 2001). The efficiency of the *Tie2-Cre*-mediated recombination of the *Foxo1*^{flox} allele was confirmed at the transcript level by qRT-PCR and at the protein level using western blots. At E8.5, *Foxo1* mRNA was significantly reduced in the conditional knockout YSs compared with control littermates, in contrast to the germline knockouts where *Foxo1* transcripts were undetectable (Fig. 1A, Fig. S1C). FOXO1 protein levels were also significantly reduced at E8.5 (Fig. 1B,C). We observed gross phenotypes in *Foxo1* conditional and global knockout mutants, similar to previous reports (Fig. 1D,E; Fig. S1A,B) (Sengupta et al., 2012; Furuyama et al., 2004; Hosaka et al., 2004). We did not detect any visible differences in vascular morphology or embryo size between control and *Foxo1*^{ECKO} at E8.5 (Fig. 1F,G). However, at E9.5 and E10.5, although the primitive vascular plexus of the control YS remodeled into a hierarchy of large caliber vessels that iteratively branched into smaller diameter capillaries, *Foxo1*^{ECKO} YSs retained a primitive vascular plexus (Fig. 1H-K). *Foxo1*^{ECKO} YSs labeled using anti-PECAM1 (CD31) antibodies, a pan EC marker, showed normal plexus at E8.5

Development (2022) 149, dev200131. doi:10.1242/dev.200131

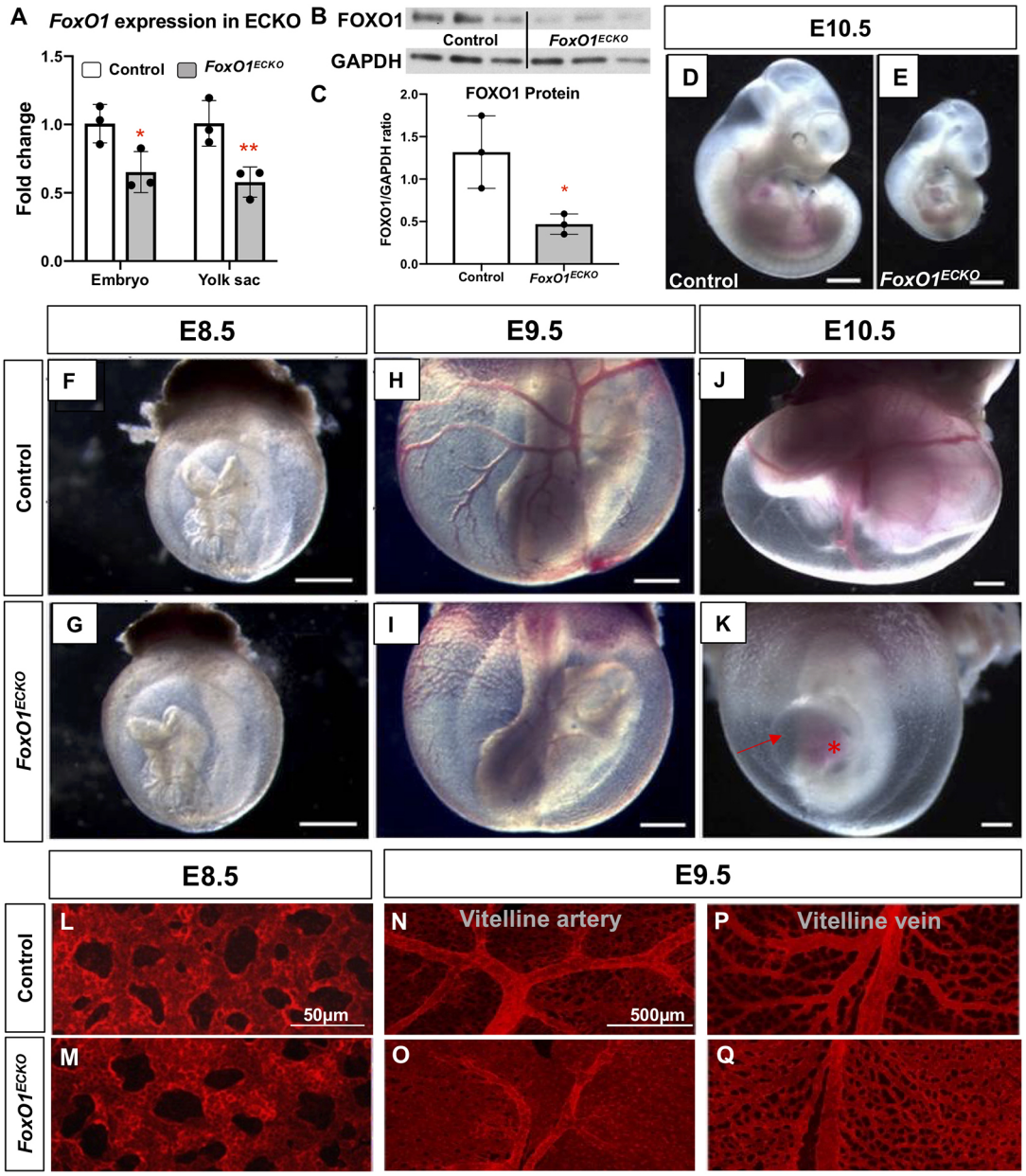

Fig. 1. *Foxo1*^{ECKO} results in vascular remodeling defects and lethality. (A) qRT-PCR for *Foxo1* expression in E8.5 control and *Foxo1*^{ECKO} YSs (**P*<0.05, ***P*<0.01). (B,C) FOXO1 protein expression in E8.5 control and *Foxo1*^{ECKO} YS (*n*=3) by western and quantification (**P*<0.05). (D,E) Bright-field images of E10.5 littermate control and *Foxo1*^{ECKO} embryos. Scale bars: 500 µm. (F-K) Control and *Foxo1*^{ECKO} embryos within the YS at E8.5 (F,G), E9.5 (H,I) and E10.5 (J,K). Scale bars: 500 µm. (K) Pericardial edema (arrow); blood pooling in the heart (asterisk). (L-Q) Pecam1 staining in E8.5 and E9.5 control and CKO YSs. Data are mean±s.d.

but thinner and less branched vitelline vein and artery compared with controls by E9.5 (Fig. 1L-Q). At E9.5, mutant embryos were reduced in overall size compared with control littermates (Fig. 1H,I), which became more evident at E10.5 (Fig. 1D,E,J,K). Additionally, in both E9.5 (not shown) and E10.5 *Foxo1*^{ECKO} embryos (Fig. 1K), the pericardial sac was enlarged, and blood was abnormally pooled in the heart. Overall, phenotypes in *Foxo1* conditional and global mutant embryos are highly reproducible and our observations align well with previously published studies (Sengupta et al., 2012; Furuyama et al., 2004; Hosaka et al., 2004), supporting the conclusion that loss of *Foxo1* in ECs and other *Tie2*-expressing cells is sufficient to cause defects in vessel remodeling.

The appearance of pericardial edema in *Foxo1*^{ECKO} embryos suggested heart failure and compromised circulation. To determine if and when blood flow was impaired, we crossed a primitive erythrocyte transgenic fluorescent reporter line, *ε-globin-KGFP* (Dyer et al., 2001), into the *Foxo1*^{ECKO} background. Live imaging of cultured embryos and high-speed confocal microscopy were used to track individual KGFP-labeled erythroblasts to determine blood velocity (Fig. 2) (Jones et al., 2004). At E8.5, both control and *Foxo1*^{ECKO} embryonic vessels were filled with blood and erythrocytes moved in a steady directional flow with similar periodicity and velocity (Fig. 2A,B,E,G). By E9.5, control embryos had clearly remodeled vessels, blood flow velocity greater than 700 µm/s and a defined wave pattern with

Development (2022) 149, dev200131. doi:10.1242/dev.200131

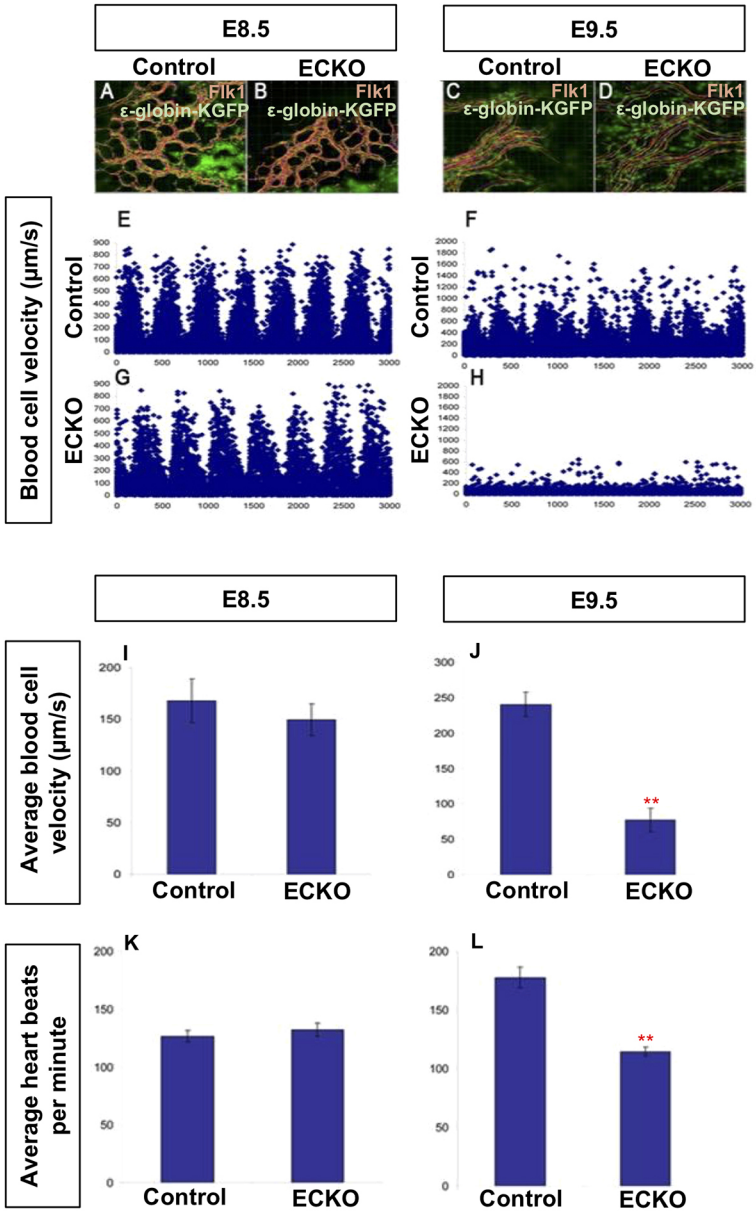

Fig. 2. Vascular remodeling defects in *Foxo1*^{ECKO} embryos do not result from reduced blood flow. Primitive erythroblasts in circulation in wild-type and CKO embryos were marked by crossing to an *ε-globin-GFP* transgenic reporter. Representative still images of E8.5 wild-type (A) and *Foxo1*^{ECKO} (B), and E9.5 wild type (C) and *Foxo1*^{ECKO} (D) embryos. (E-H) Individual blood cells from A-D were tracked and velocity profiles are plotted. (I,J) Quantification of the average blood velocity (Mann–Whitney *U*-test, ***P*=0.005). Average heart rates quantified in wild-type and *Foxo1*^{ECKO} embryos at E8.5 (K) and E9.5 (L) (Kruskal–Wallis test, ***P*=0.003). Data are mean± s.e.m.

periodicity of 400 ms (Fig. 2C,F). However, *Foxo1*^{ECKO} embryos vessels were not remodeled, and blood flow had a significantly lower velocity with a poorly defined wave pattern (Fig. 2D,H). Quantification of blood velocity (Fig. 2I,J) and heart rate (Fig. 2K,L) revealed no statistical difference in E8.5 control and *Foxo1*^{ECKO} embryos (Fig. 2I,K). However, by E9.5, blood velocity and heart rate were significantly decreased in *Foxo1*^{ECKO} embryos (Fig. 2J,L), indicating heart failure was occurring in embryos with un-remodeled vessels. Thus, flow initiates normally in *Foxo1*^{ECKO} embryos, but defects in both vascular remodeling and blood flow abnormalities were observed by E9.5. Given these results, we restricted our analysis, whenever possible, to E8.25 (the 4- to 7-somite range) embryos so that poor blood flow did not influence our data.

A previous report on the role of *Foxo1* in placental development described phenotypes including swollen or hydropic allantois, failed chorion-allantoic fusion, and increased cell death in the allantois (Ferdous et al., 2011). Since the previous study was conducted in germline *Foxo1* null embryos, we examined the allantois in global null and *Foxo1*^{ECKO} mutants. While germline *Foxo1* mutants exhibited partially penetrant defects in allantois formation and fusion, these phenotypes were not evident in *Foxo1*^{ECKO} embryos at E9.5 (Table 1). However, both germline and *Foxo1*^{ECKO} embryos show defects in YS vascular remodeling, heart failure phenotypes, and lethality by E11.5. Taken together, these results support a cell autonomous requirement for FOXO1 in YS vessel remodeling and suggest that published cardiac and blood flow defects are secondary to the impaired remodeling of YS vasculature.

FOXO1 is necessary to maintain *Flk1* expression in E8.25 YSs

To assess mechanisms disrupted in *Foxo1*^{ECKO}, we examined transcript levels of genes normally expressed in blood vessels by qRT-PCR within *Foxo1*^{ECKO} E8.25 YSs. We focused these experiments at E8.25 prior to vessel remodeling and to avoid potential complications of later stage heart failure. We observed a significant decrease in *Flk1* expression in *Foxo1*^{ECKO} YSs, while other pan-endothelial markers, such as *Pecam1*, *Tie2*, VE-cadherin

Development (2022) 149, dev200131. doi:10.1242/dev.200131

Table 1. Allantois phenotype analysis in control, null and *Foxo1*^{ECKO} embryos at E9.5

	Genotype	Number of embryos	Percentage of total	Number with gross allantois defects	Percentage of genotype
Germline	Wild type	16	31.37	0	N/A
Four litters	*Foxo1*$^{+/null}$	20	39.22	0	N/A
	Foxo1$^{null/null}$	15	29.41	2	13.33
	Total	51			
Conditional	*Foxo1*$^{+/flox}$	15	31.91	0	N/A
Six litters	*Foxo1*$^{+/flox}$;*Tie2-cre*$^{+/Tg}$	12	25.53	0	N/A
	Foxo1$^{flox/flox}$	10	21.28	0	N/A
	Foxo1$^{flox/flox}$;*Tie2-cre*$^{+/Tg}$	10	21.28	0	N/A
	Total	47			

N/A, not applicable.

(*Cdh5*), *Flt1* (also known as *Vegfr1*) and *Cx43* (*Gja1*) were not significantly affected (Fig. 3A). Consistent downregulation of *Flk1* was also seen in the *Foxo1* global knockout YSs and no change in *Flk1* expression was detected in the embryo proper (Fig. S2A). Immunolabeling of endogenous *Flk1* showed a similar reduction in expression in *Foxo1*^{ECKO} YS ECs at E8.25, while PECAM1 (CD31) expression appeared unaffected (Fig. 3B). We further confirmed the reduction in *Flk1* expression using magnetic-activated cell sorting (MACS) to isolate CD31^{+} cells (primarily ECs) from E8.25 wild-type and *Foxo1* germline deletion mutant YSs. CD31^{+} YS cells showed sevenfold higher *Pecam1* (CD31) expression than whole YSs (sorted then recombined) and ∼30-fold higher than the CD31^{-} population, demonstrating high-fidelity enrichment via MACS (Fig. 3C). To compare wild-type and mutant YS ECs, we assayed transcript levels of both *Pecam1* and *Flk1* in the CD31^{+} populations. *Pecam1* levels were comparable between wild-type and mutant CD31^{+} cells, whereas *Flk1* was significantly reduced in the null CD31^{+} population (Fig. 3D,E). Finally, we examined *Flk1* expression using a transgenic reporter, *Flk1-H2B::YFP* (Fraser et al., 2005), that labels EC nuclei. At E8.25, YFP^{+} endothelial nuclei were evenly dispersed throughout the vascular plexus of control YSs; however, the number of YFP^{+} nuclei within the *Foxo1*^{ECKO} YSs were significantly reduced (Fig. 3F). The total number of DAPI^{+} nuclei was unchanged. Nuclear segmentation and quantification of the average YFP^{+} cell density revealed a significant reduction in the number of YFP^{+} cells in *Foxo1*^{ECKO} YSs compared with controls (Fig. 3G). To determine whether the reduction in YFP^{+} cells was due to a difference in apoptosis or proliferation, *Foxo1*^{ECKO} litters positive for the *Flk1-H2B-YFP* reporter were immunostained for phospho-histone 3 (PH3) or caspase 3 (Fig. 3H,I). We found that neither cell proliferation nor apoptosis within the YS differed significantly between control and *Foxo1*^{ECKO} embryos (Fig. 3H,I, Fig. S2B-E). As the mRNA expression of pan-endothelial markers was not decreased, but FLK1 transcripts and protein were reduced, we concluded that the low density in YFP^{+} cells is not due to reduced EC numbers, but rather to reduced expression of the *Flk1* reporter. Collectively, these data indicate that FOXO1 is required to maintain cell autonomous *Flk1* expression in ECs, but not required for the formation, proliferation or survival of ECs, or the expression of other pan-endothelial markers.

FOXO1 is required to regulate arterial gene expression in the YS vasculature

Given the reduced *Flk1* expression in E8.25 YSs, and the crucial role of VEGF-VEGFR2 signaling in establishing arteriovenous identity in the early embryonic endothelium, we next examined other AV specification markers (Fig. 4A). Previously, Furuyama et al. showed reduced arterial-enriched transcripts *Cx40* (*Gja5*), *Cx37* (*Gja5*), *eNOS* (*Nos3*) and ephrin B2 (*Efnb2*) in E9.5 *Foxo1*^{ECKO} YSs compared with control littermates (Furuyama et al., 2004), but given the changes in blood flow that we observed in E9.5 *Foxo1*^{ECKO} embryos, we were interested to determine whether expression of these markers was affected earlier. Indeed, these genes were significantly reduced in *Foxo1*^{ECKO} YSs at E8.25 compared with controls (Fig. 4A). In addition, we found a significant reduction in Notch family member transcript levels, including *Notch1*, *Hey1*, jagged 1 (*Jag1*) and *Dll4*, which are required for arterial specification (Gridley, 2010; Duarte et al., 2004; Xue et al., 1999; Fischer et al., 2004). Venous markers, neuropilin 2 (*Nrp2*), Coup-TFII (*Nr2f2*) and *Ephb4* showed no significant change (Wang et al., 1998; You et al., 2005). The endodermal marker *Afp* was also unchanged (Fig. 4A) (Dziadek and Adamson, 1978). These results demonstrate that FOXO1 is required for normal early arterial gene expression in the murine YS.

To determine whether reduced arterial-specific gene expression correlated with decreased expression of their respective proteins in *Foxo1*^{ECKO} YSs, immunofluorescence was performed on sectioned YSs at E8.5 and E9.5. Confocal imaging of Cx37 and Cx40 revealed an overall reduction in the number of connexin-positive puncta in *Foxo1*^{ECKO} YSs when compared with controls at both stages (Fig. S3A and B). Similarly, we observed decreased eNOS expression within the vascular plexus in *Foxo1*^{ECKO} yolks sacs compared with controls (Fig. 4B). These data, in addition to previous gene expression analysis, indicate that FOXO1 within the developing endothelium is necessary for the regulation of arterial identity.

Characterization of arterial defects in *Foxo1*^{ECKO} and germline mutants using the *Dll4-BAC-nlacZ* reporter

Thus far, our phenotypic, transcriptional and immunolabeling studies support a role for FOXO1 in regulating vascular remodeling, *Flk1* expression and arterial specification of ECs within the YS. To further analyze the arterial specification defects in *Foxo1*^{ECKO} mutants, we examined the spatial expression of one of the earliest markers of arterial identity (Chong et al., 2011; Wythe et al., 2013), *Dll4*, using a transgenic reporter line, *Dll4-BAC-nlacZ*, that faithfully recapitulates endogenous *Dll4* expression (Herman et al., 2018). E8.25 *Foxo1*^{ECKO} embryos carrying the nuclear-localized β-galactosidase reporter were compared with control littermates (Fig. 5 and Fig. S4). In E8.25 control embryos, *Dll4-BAC-nlacZ* reporter activity was observed in the dorsal aorta (DA), endocardium (EN) and nascent umbilical artery (UA) within the allantois (Fig. 5A and Fig. S4A). LacZ-positive nuclei were also detected within the YS in and around the vitelline artery and arterioles (Fig. 5A, red arrows). *Foxo1*^{ECKO} YSs exhibited a similar LacZ expression pattern spatially, albeit with reduced intensity (Fig. 5B), consistent with our transcript analysis showing reduced *Dll4* mRNA expression in the *Foxo1*^{ECKO} YSs

Development (2022) 149, dev200131. doi:10.1242/dev.200131

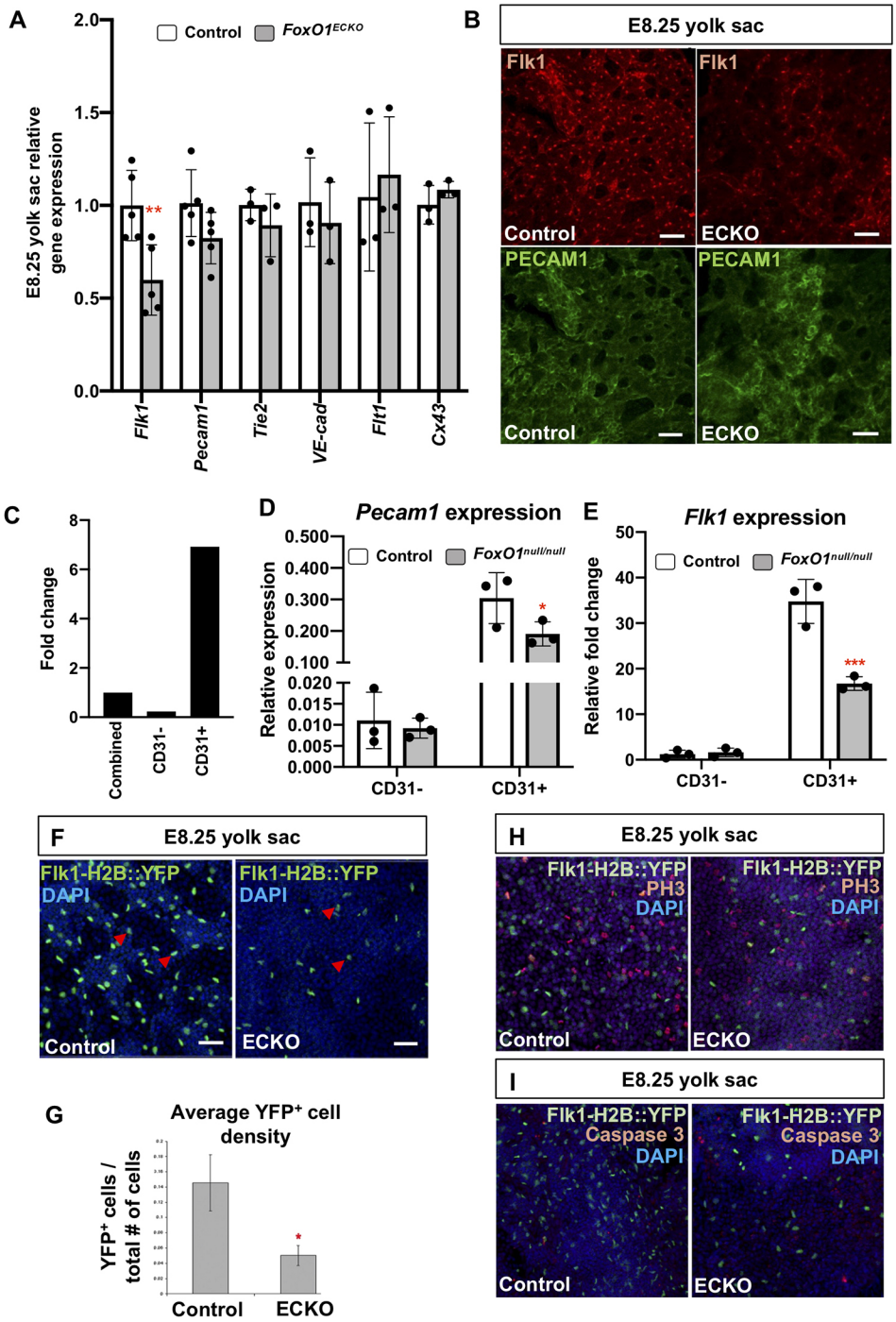

Fig. 3. FOXO1 regulates FLK1 expression without affecting other endothelial genes or EC viability prior to blood flow. (A) Expression levels of endothelial genes by quantitative RT-PCR. (B) Immunolabeling for endogenous FLK1 and PECAM1 in control and *Foxo1*^{ECKO} YSs. Scale bars: 50 µm. (C) Comparison of *Pecam1* expression in MACS-sorted CD31^{-}, CD31^{+} and combined control E8.25 YS cells by qPCR. (D,E) Relative *Pecam1* (D) and *Flk1* (E) expression between wild-type and *Foxo1*^{null} E8.25 MACS-sorted CD31^{-} and CD31^{+} YS cells. (F) YSs from control and *Foxo1*^{ECKO} at E8.25 DAPI stained and positive for *Flk1-H2B::YFP* transgene, which marks the EC nuclei (arrowheads). (G) Quantification of YFP^{+} cells relative to total number of cells labeled with DAPI from F. (H,I) Whole-mount phosphor-Histone-H3 (PH3) (H) or activated caspase 3 (I) staining of control and *Foxo1*^{ECKO} E8.25 YSs co-labeled with *Flk1-H2B::YFP* transgene and DAPI. Data are mean±s.d. (n=3). *P<0.05, **P<0.01, ***P<0.001.

(Figs 4A and 5C). However, unlike in the YS, nLacZ expression was only slightly reduced in the embryo proper of *Foxo1*^{ECKO} mutants (Fig. S4B compared with Fig. S4A, Fig. 5C). To determine whether the differences in nLacZ reporter expression between the YS and embryo was influenced by Cre-mediated recombination in our conditional knockout studies, we examined the activity of the *Dll4* LacZ reporter in germline *Foxo1* mutants. Fig. S4E,F show representative images of anterior views of the embryos, while Fig. 5D,E show posterior views. *Foxo1*$^{null/null}$ showed even greater decreases in reporter expression compared with control YSs and embryos (Fig. 5D,E, red arrows). A small but significant decrease in endogenous *Dll4* expression was seen between wild-type and *Foxo1*$^{null/null}$ embryos (Fig. 5F). Whereas, a dramatic reduction in *Dll4* expression was observed in the *Foxo1* null YSs compared with wild-type controls (Fig. 5F).

By E9.5, nLacZ reporter expression was detected in the arterial tree in the YS, particularly in the VA and within the arterioles (Fig. 5G). Consistent with the E8.25 results, we found *Dll4* expression reduced in E9.5 *Foxo1*^{ECKO} YSs (Fig. 5H) but strong expression in vessels within control and *Foxo1*^{ECKO} embryos (Fig. 5I,J). Germline null embryos showed similar nLacZ activity compared with controls (Fig. 5K), but reporter expression was not detectable in null YSs, despite the strong expression seen in the embryo (Fig. 5L). Isolated embryos confirmed LacZ expression in

Development (2022) 149, dev200131. doi:10.1242/dev.200131

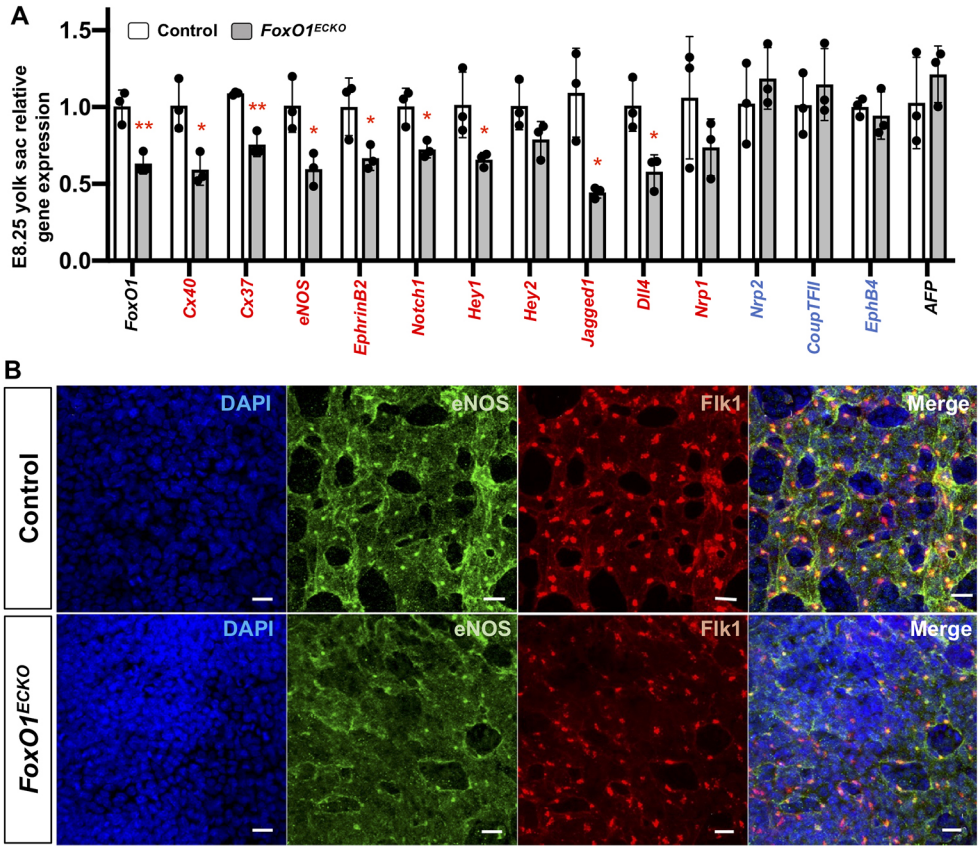

Fig. 4. Arterial marker expression is reduced in *Foxo1*^{ECKO} YS. (A) qRT-PCR expression analysis in control and *Foxo1*^{ECKO} YSs; arterial (red), venous (blue) and endoderm markers at E8.25. **P*<0.05, ***P*<0.01; data are mean±s.d. (*n*=3). (B) Co-immunolabeling of eNOS, FLK1 and DAPI in control and *Foxo1*^{ECKO} YSs at E8.25. Scale bars: 20 µm.

both control (Fig. 5M) and null embryos (Fig. 5N). Additional analysis of *Dll4* reporter expression confirmed previous reports of vascular defects in *Foxo1* mutants, including within the intersomitic vessels, cranial vessels and dorsal aorta (Fig. 5I,J,M,N, red arrows) (Hosaka et al., 2004; Ferdous et al., 2011; Dharaneeswaran et al., 2014). Collectively, our results indicate that FOXO1 plays a crucial and early role in the regulation of *Dll4* expression, a key factor in determining arterial identity, within the extra-embryonic arteries of the YS, but does not appear to be required for *Dll4* expression within the embryo proper.

Conditional *Foxo1* deletion upregulates *Spry2* and *Spry4* expression

We uncovered a novel role for FOXO1 in the establishment of arterial identity, but neither *Flk1* nor *Dll4* contains known binding sites for FOXO1; thus, we examined expression levels of previously validated direct transcriptional targets of FOXO1 in the endothelium: adrenomedullin (*Adm*), BMP binding endothelial regulator (*Bmper*), *Nos3*, *Spry2* and *Vcam1* (Potente et al., 2005; Ferdous et al., 2011). qRT-PCR analysis in *Foxo1*^{ECKO} YSs at E8.25 (Fig. 6A) revealed no significant reduction in *Adm* or *Bmper*, but a significant downregulation in *Nos3* and *Vcam1* compared with controls, as previously described in other tissues (Potente et al., 2005; Ferdous et al., 2011). Interestingly, *Foxo1*^{ECKO} YSs showed significantly increased *Spry2* expression (Fig. 6A). Subsequent analysis showed that in addition to *Spry2*, *Spry4* was also upregulated in mutant YSs compared with controls, while *Spry1* and *Spry3* levels were unchanged (Fig. 6B). The upregulation in *Spry2* and *Spry4* is specific to the YS as no significant changes in sprout gene expression were seen in the embryo proper (Fig. S5). We focused our subsequent analysis on the Spry factors because Spry4 overexpression has been shown to inhibit angiogenesis in the YS (Lee et al., 2001) and the upregulation of sprouty transcripts in *Foxo1*^{ECKO} led us to hypothesize that FOXO1 may act as a direct repressor of sprouty gene expression.

In keeping with the idea that FOXO1 may normally repress *Spry 2* and *Spry4* transcription, we examined endogenous mRNA levels of *Foxo1*, *Spry1*, *Spry2*, *Spry3* and *Spry4* in wild-type E8.25-8.5 YSs. This analysis revealed that *Spry2* and *Spry4* expression is much lower than *Foxo1*, *Spry1* or *Spry3* (Fig. 6C). To expand and confirm endothelial specificity of our previous *Spry2* and *Spry4* expression analysis, we examined *Spry2* and *Spry4* transcripts in CD31$^+$ and CD31$^-$ MACS-sorted cells from germline *Foxo1* mutants and wild-type YSs (Fig. 3D). For *Spry2*, we observed increased expression in YS CD31$^+$ cells, but there was no change in CD31$^-$ cells from null mutant YSs (Fig. 6D). Surprisingly, although *Spry4* transcripts were increased in CD31$^+$ cells of null YSs, transcripts were decreased in the CD31$^-$ population. These data suggest that FOXO1 may act as both a transcriptional repressor or activator in adjacent tissues in the YS, depending on the cell identity or transcriptional target.

FOXO1 directly binds to endogenous *Spry2* and *Spry4* promoters and represses *Spry2* and *Spry4* transcription

FOXO1 is known to regulate *Spry2* mRNA expression in liver ECs, and *in vivo* chromatin immunoprecipitation (ChIP) experiments confirmed that FOXO1 occupies four conserved FOXO-binding elements within the murine *Spry2* locus (Paik et al., 2007). The first FOXO1-binding site (Fig. S5A) is located ~4 kb upstream of the transcriptional start site (TSS) of murine *Spry2*; the second DNA-binding site is within exon 2 (Fig. 7A). The third and fourth FOXO1 binding sites are located ~5 kb and 7 kb downstream of the TSS,

Development (2022) 149, dev200131. doi:10.1242/dev.200131

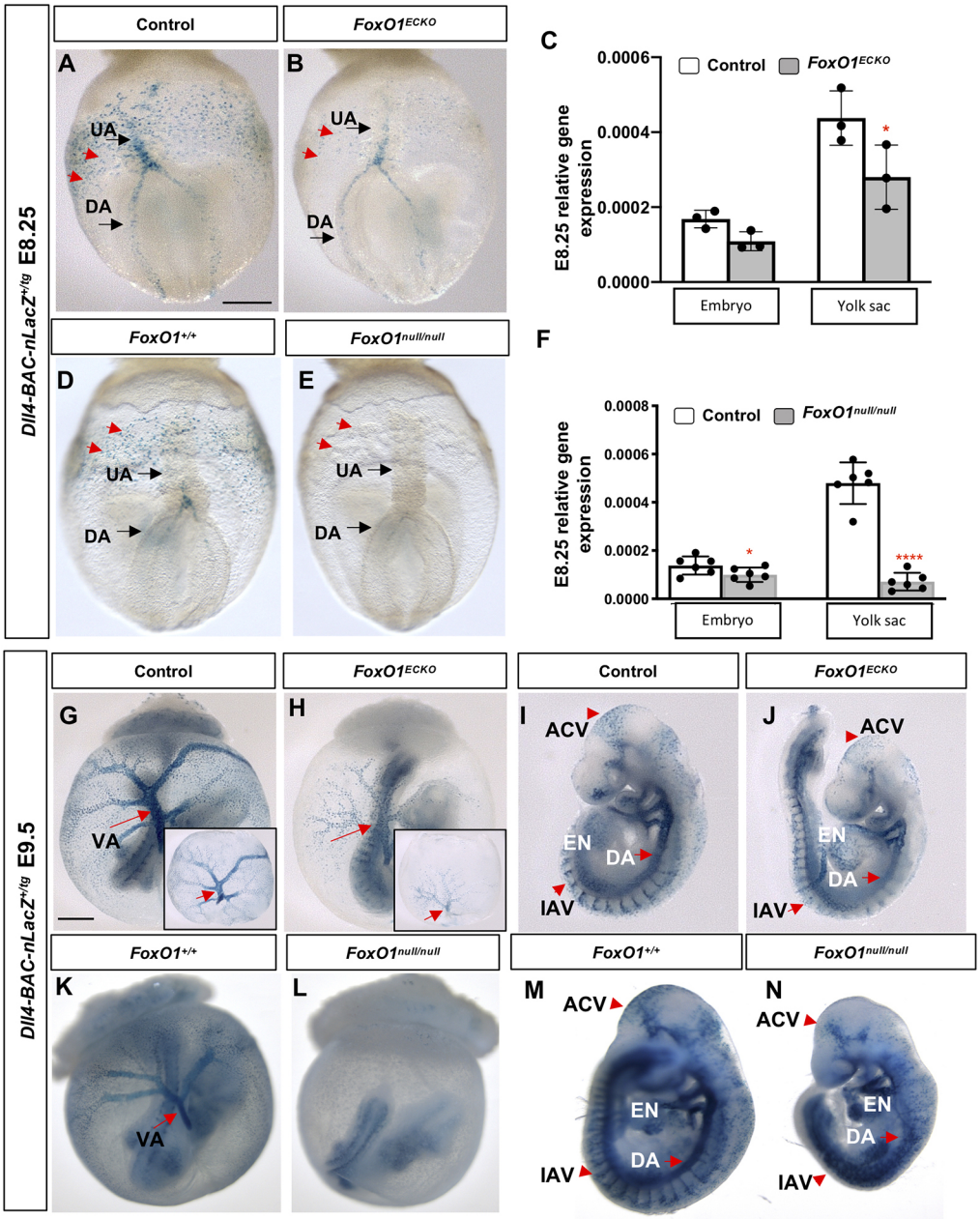

Fig. 5. Characterization of arterial defects in *Foxo1*^{ECKO} and germline mutants. (A,B,D,E) Using the *Dll4-BAC-nlacZ* reporter, *nlacZ* reporter activity was detected in the dorsal aorta (DA) and umbilical artery (UA) in E8.25 littermate control, *Foxo1*^{ECKO} and *Foxo1*-null embryos. Red arrows indicate YS ECs in the posterior region of the YS plexus. (C,F) qRT-PCR for *Dll4* mRNA expression in littermate control, *Foxo1*^{ECKO} and *Foxo1*-null embryos and YSs (n>3; *P<0.05, ****P<0.0001). Data are mean±s.d. (G,H,K,L) *nlacZ* reporter activity in E9.5 littermate control, *Foxo1*^{ECKO} and *Foxo1*-null YS and embryo. VA, vitelline artery (arrows); insets in G and H show YSs only. (I,J,M,N) *nlacZ* reporter activity in E9.5 littermate control, *Foxo1*^{ECKO} and *Foxo1*-null embryos. EN, endocardium; DA, dorsal aorta; IAV, intersomitic arterial vessels; ACV, arterial cranial vasculature. Scale bars: 200 µm (E8.25); 500 µm (E9.5).

respectively (Fig. 7A). Paik et al. showed that FOXO1 interacts with these loci to activate *Spry2* in the liver, but it was unknown whether FOXO1 uses the same binding sites to repress *Spry2* in the YS. To determine whether FOXO1 occupies any of these four identified binding sites in the murine YS, we performed ChIP-PCR using pooled wild-type E8.25 YSs. As shown in Fig. 7B, FOXO1 occupancy was significantly enriched at the −4051, +5060 and +6972 regions compared with IgG control. FOXO1 enrichment was not observed at the +4479 region. This demonstrates that, during early YS vessel development, FOXO1 binds *Spry2* at regulatory regions −4051, +5060 and +6972, and supports the context-dependent function of FOXO1.

Next, we generated luciferase reporter constructs containing ~2 kb of the murine *Spry2* promoter or specific regulatory regions harboring FOXO1-binding sites, and measured transcriptional activity in cultured mammalian cells (Fig. S6B). To avoid potential confounds in our analysis from endogenous FOXO1, the human lung cancer cell line H1299 was chosen as FOXO1 protein expression is undetectable in this line (Zhao et al., 2010). Overexpression of *Foxo1* (*FLAG::Foxo1*) significantly repressed luciferase activity of the promoter construct containing the −4051 FOXO1-binding site in a dose-dependent manner. Furthermore, co-transfecting the same reporter construct along with a FOXO1 cDNA without a DNA-binding domain abolished this transcriptional repression (Fig. 7C). In contrast, FOXO1 did not significantly repress luciferase activity in the constructs containing either the +4479/5060 combined or +6972 *Spry2* regulatory regions (Fig. 7C). These results suggest that FOXO1 directly downregulates *Spry2* expression via the −4051 site in its promoter.

To determine whether this role for FOXO1 is evolutionarily conserved, we examined the *Spry4* locus for conserved FOXO1 DNA-binding motifs (Fig. S6A). Two putative binding sites, which were conserved in at least three vertebrate genomes (mammalian and non-mammalian), were identified +8755 bp and +14,942 bp

Development (2022) 149, dev200131. doi:10.1242/dev.200131

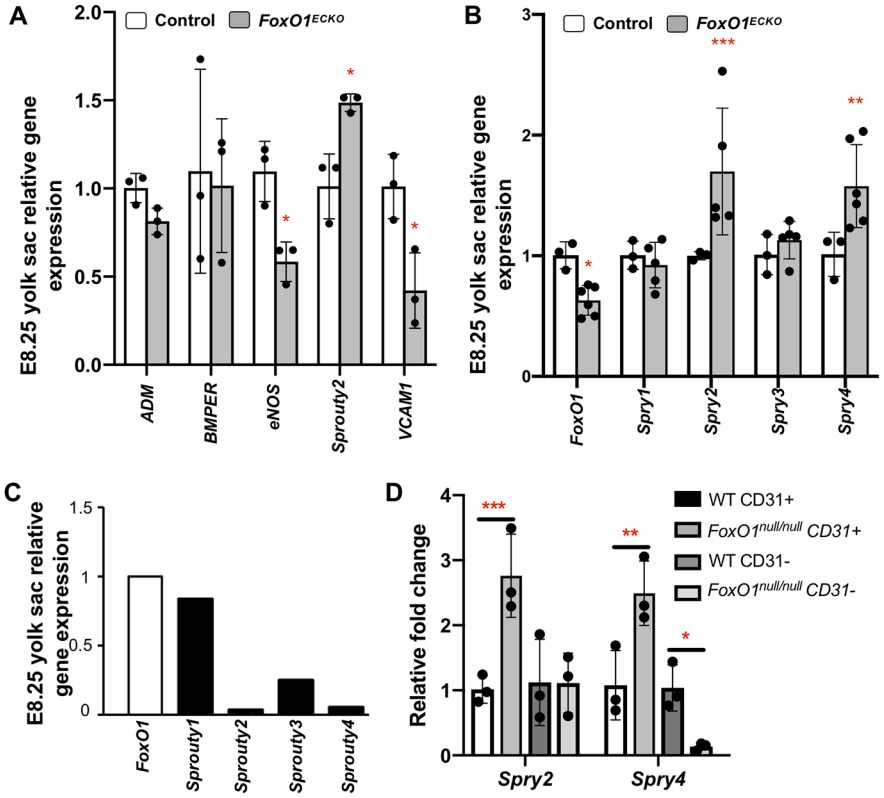

Fig. 6. FOXO1 regulates *Spry2* and *Spry4* expression in the YS vasculature. (A,B) qRT-PCR analysis in littermate E8.25 control and *Foxo1*^{ECKO} YSs for (A) known FOXO1 targets and (B) *Spry* family members. (C) qRT-PCR of endogenous *Spry1*, *Spry2*, *Spry3* and *Spry4* expression relative to *Foxo1*. (D) Quantitative RT-PCR of *Spry2* and *Spry4* in MACS-sorted E8.25 CD31$^+$ and CD31$^-$ control and *Foxo1*^{null} YS cells. Data are mean±s.d. (n=3). *P<0.05, **P<0.01, ***P<0.001.

downstream of the *Spry4* TSS (Fig. 7D). FOXO1 ChIP-PCR using E8.25 YS chromatin showed a significant enrichment of FOXO1 occupancy in both regulatory regions (Fig. 7E). Luciferase assays in H1299 cells also showed that these same sites were required for wild-type FOXO1 dose-dependent repression of reporter activity (Fig. 5F and Fig. S6C). Taken together, data from the *Spry* mRNA expression analysis, as well as ChIP and luciferase assays, demonstrated that FOXO1 directly repressed *Spry2* and *Spry4* transcription in the E8.25 murine YS via known and newly identified conserved DNA-binding sites.

Transient overexpression of *Spry4* in ECs partially phenocopies conditional loss-of-function *Foxo1* mutants

Spry2 and *Spry4* are known to have anti-angiogenic functions (Taniguchi et al., 2009; Wietecha et al., 2011; Lee et al., 2001), and our data here show that FOXO1 directly represses *Spry2* and *Spry4* expression in the YS, we hypothesized that FOXO1 promotes arterial gene expression by repressing *Spry2* and *Spry4*. It had previously been shown that adenovirus-mediated overexpression of *Spry4* in developing embryos inhibited sprouting and branching of small vessels in the embryo proper and vessel remodeling in the YS (Lee et al., 2001). To test whether *Spry4* overexpression could recapitulate the *Foxo1* loss-of-function phenotype, we used a well-characterized *Flk1* promoter-enhancer construct that is expressed in YS and embryonic ECs (Kappel et al., 1999; Rönicke et al., 1996; Fraser et al., 2005) to transiently overexpress *Spry4* beginning at E7.5. To track transgene expression, a H2B::YFP reporter was inserted downstream to enable YFP$^+$ transgenic embryo identification (schematized in Fig. 8A). At E9.5, YSs of YFP$^+$ transgenic embryos (n=3) showed poorly remodeled vasculature, as their vessels remained as a primitive vascular plexus, while non-transgenic embryos had a normally developed vitelline artery with large caliber vessels branching into smaller diameter capillaries (Fig. 8B). The lack of YS vascular remodeling in the transient transgenic *Flk1-Spry4* embryos phenocopied the vascular remodeling defects in *Foxo1*^{ECKO} embryos and was similar to previous loss-of-function data (Lee et al., 2001). YSs harvested from both transgenic and control embryos confirmed the expression of YFP transcripts and exogenous *Spry4* only in transgenic embryos (Fig. S7).

Next, we used total RNA from transgenic YFP$^+$ and control YSs and embryos that were within E8.25 4-7 somite stage for analysis. The relative expression level of each arterial marker was first normalized *Gapdh*, the internal control, then to endogenous *Spry4* in order to compare the effect of exogenous *Spry4* overexpression. Transcript levels were compared between control and YFP$^+$ transgenic groups. Arterial markers, such as *Cx37*, *Efnb2*, *Notch1*, *Hey1*, *Jag1* and *Dll4* were significantly downregulated in the YSs of transgenic embryos compared with controls (Fig. 8C), whereas expression within the embryo proper of these markers was not significantly changed, apart from *Jag1* (Fig. 8D). *Cx40* expression was not significantly different between the control and transgenic groups in either the YS or embryos (Fig. 8C,D). Additionally, unlike in *Foxo1*^{ECKO} YSs, expression of venous marker *Ephb4* was significantly downregulated in the YS and *Nr2f2* expression was significantly increased in the transgenic embryos. The broader effects produced by *Spry4* overexpression directed by the *Flk1* promoter/enhancer could indicate that SPRY4 has FOXO1-independent functions, or that abnormally high levels of *Spry4* may affect other processes. These data, combined with our results showing that FOXO1 represses *Spry2* and *Spry4* transcription, indicates that FOXO1 acts as a key transcriptional regulator in AV specification by repressing an antagonist of arterial specification.

DISCUSSION

Previously, using either germline mutations or conditional approaches, several groups demonstrated a requirement for

Development (2022) 149, dev200131. doi:10.1242/dev.200131

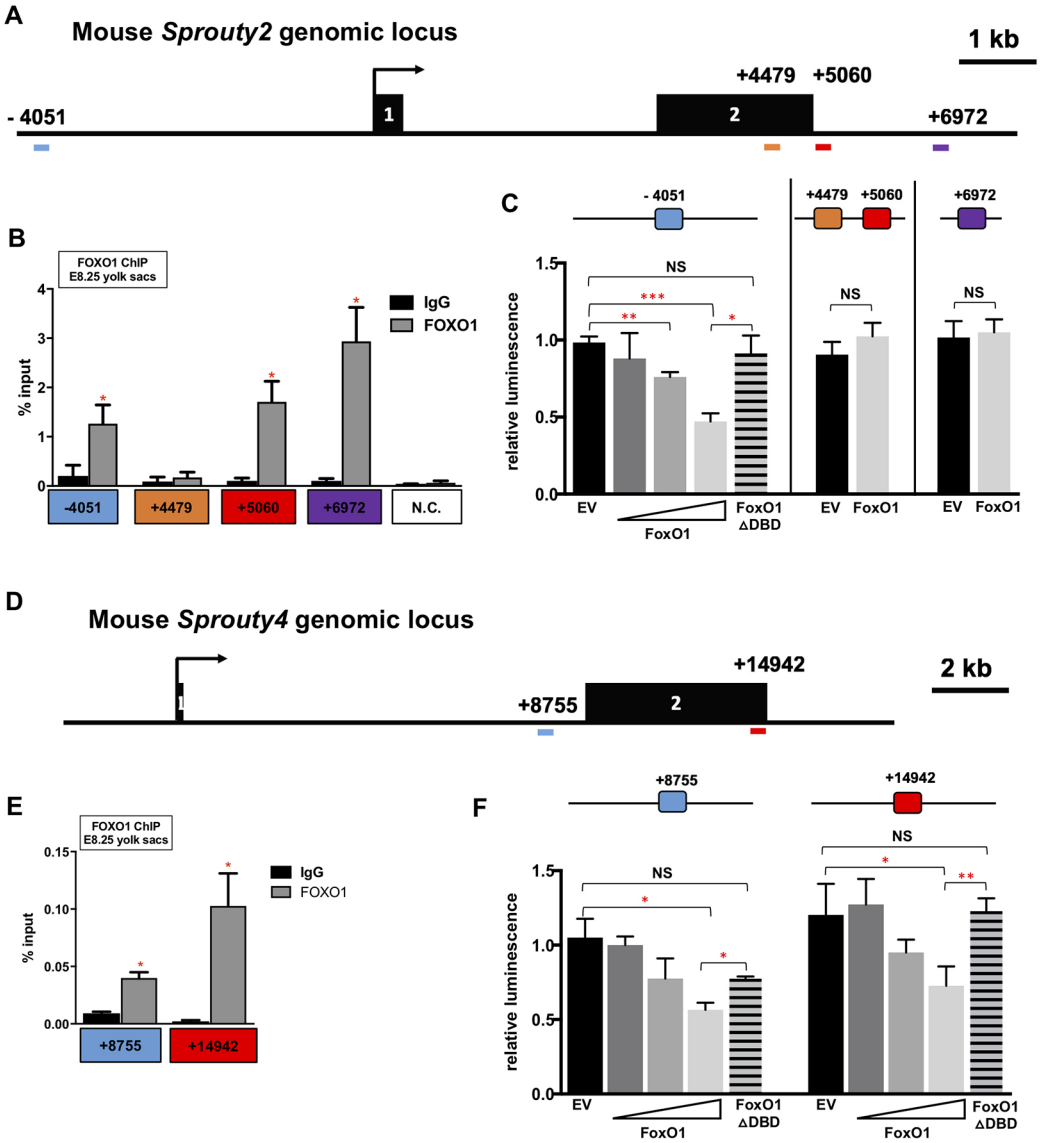

Fig. 7. FOXO1 directly binds to endogenous *Spry2* and *Spry4* promoters, and represses *Spry2* and *Spry4* transcription. (A) Genomic locus of mouse *Spry2* gene with the FOXO1-binding sites in blue, orange, red and purple. (B,E) FOXO1 ChIP-PCR using E8.25 YS chromatin. (C) Luciferase activity of FOXO1 on the *Spry2* promoter in H1299 cells. (D) Genomic locus of mouse *Spry4* gene with the FOXO1-binding sites in blue and red. (F) Luciferase activity of FOXO1 on the *Spry4* promoter in H1299 cells. **P*<0.05, ***P*<0.01, ****P*<0.001. EV, empty vector. Data are mean±s.d.

FOXO1 in the early embryo, as these mutants featured failed YS remodeling and mid-gestation lethality (Sengupta et al., 2012; Furuyama et al., 2004; Hosaka et al., 2004). In this paper, we investigated the role of FOXO1 within the YS vascular plexus prior to the onset of consistent circulation and overt vascular remodeling. It is well known that arteriovenous specification and the arterial gene expression program are influenced by hemodynamic forces (le Noble et al., 2004, 2005; Wragg et al., 2014), but our goal here was to determine whether FOXO1 functions before the onset of hemodynamic signaling to affect arteriovenous patterning. Herein, we demonstrate that blood flow is normal in *Foxo1*^{ECKO} mutants at these early stages, although heart failure and poor circulation are evident by E9.5 (Fig. 2). Others have shown that FOXO1 is not required for heart development (Sengupta et al., 2012), and it is possible that heart failure in these embryos is caused by the increased resistance of blood flow encountered in the unremodeled vitelline vessels. Additionally, loss of FOXO1 causes allantois defects, preventing normal allantois fusion and circulation to the placenta (Ferdous et al., 2011). We did not observe overt defects in allantois fusion in *Foxo1*^{ECKO} embryos (0/10 *Foxo1*$^{flox/flox}$;*Tie2-cre*$^{Tg/+}$) (Table 1) and observed only low penetrance of allantois fusion defects (2/15) in the germline *Foxo1* knockout embryos, whereas all fully null or *Foxo1*^{ECKO} embryos examined showed defects in YS remodeling, heart failure and mid-gestation lethality. Thus, it is likely that the heart failure and lethality are caused by increased resistance to blood flow in vitelline vessels; however, the reduction in *Dll4* expression that we observed using the *Dll4-BAC-nlacZ* reporter in *Foxo1*^{ECKO} and germline null mutants suggests that further investigation of the consequence *Dll4* loss in allantois development is warranted.

In this study, we report that FOXO1 plays a previously unidentified role in regulating arterial-specific gene expression prior to the onset of blood flow. Based on transcript expression analyses, immunostaining and transgenic reporter experiments, we

Development (2022) 149, dev200131. doi:10.1242/dev.200131

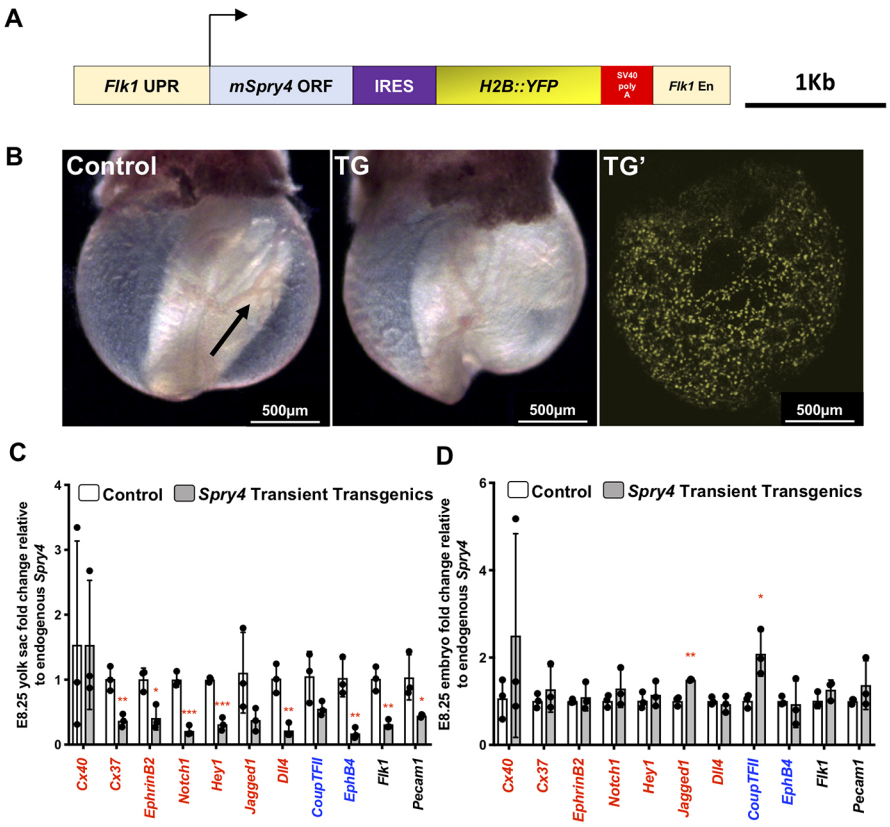

Fig. 8. Transient overexpression of *Spry4* in ECs partially phenocopies *Foxo1*^{ECKO} mutants. (A) Schematic of *Spry4* overexpression construct for pro-nuclei injection. (B) Bright-field image of E9.5 non-transgenic (control) and a transgenic embryo (TG). Confocal imaging of a TG embryo (TG′) showing YFP fluorescence in YS. Vessel remodeling in the control YS (arrow). (C,D) qRT-PCR of arterial markers in E8.25 control and TG YSs (C) and embryos (D) (n=3). *P<0.05, **P<0.01 and ***P<0.001. Data are mean±s.d.

have concluded that loss of *Foxo1* causes a significant downregulation in *Flk1* and crucial arterial markers, including *Dll4*, in the YS without affecting cell proliferation or cell death. Furthermore, our data demonstrate that FOXO1 directly binds to *Spry 2* and *Spry4* regulatory regions in the YS, and that FOXO1 acts as a direct repressor of *Spry 2* and *Spry4* in YS cells. Finally, we show that overexpression of *Spry4* in ECs *in vivo* was sufficient to recapitulate impairments in both the vascular remodeling at E9.5 and arterial cell fate specification at E8.25 seen in *Foxo1* mutants. These data, combined with our results showing that FOXO1 represses *Spry2* and *Spry4* transcription, indicate that FOXO1 acts as a key transcriptional regulator in AV specification by repressing an antagonist of arterial specification. However, given the caveat that we also observed disruptions to venous marker expression in *Spry 4* overexpression embryos, it is not yet clear whether sprouty factors participate only in limiting arterial gene expression or whether they play a broader role in early EC specification.

Our studies support a model where FOXO1 represses *Spry2* and *Spry4* in YS ECs to promote early arterial specification in the YS prior to the onset of robust embryonic circulation. Interestingly, although we observed elevated *Spry2* and *Spry4* transcripts in YS CD31^{+} cells of *Foxo1* null embryos, we found reduced *Spry 4* mRNA expression in CD31^{-} cells in the YS, suggesting FOXO1 may act as activator for *Spry4* in other cell types of the YS. Recent studies showed that FOXO1 functions as a transcriptional repressor in hepatocytes (Langlet et al., 2017) and pancreatic progenitor cells (Jiang et al., 2017). In some instances, different co-factors have been identified that enable FOXO1 to act as an activator or a repressor in different cell types of the same tissues (Langlet et al., 2017). A similar mechanism may explain the observed differences between endothelial and non-ECs within the YS. It is not yet known whether a transcriptional co-factor in YS ECs is required for FOXO1 to act as a repressor, or whether another mechanism accounts for the opposite regulation of *Spry4* in adjacent cell layers. It is also not yet clear whether the downregulation of *Spry4* in the CD31^{-} cells has a functional consequence. Further work is needed to determine whether Sprouty factors play multiple roles in early yolk sac development.

Foxo1 loss did not appear to affect normal expression of pan-endothelial markers *Pecam1* and *Tie2*, and other genes, but *Flk1* was significantly reduced in both *Foxo1*^{ECKO} YS and sorted germline mutant YS CD31^{+} cells. We also found that despite the reduction in *Flk1*, we did not observe changes in cell proliferation or cell viability, two process that are directly regulated by VEGF-VEGFR signaling (Bernatchez et al., 1999). Sprouty factors inhibit receptor tyrosine kinase signaling, and sprouty overexpression could cause a reduction in *Flk1* that is normally promoted by FLK1 or FGF receptor activation (Lee et al., 2001; Casci et al., 1999). Indeed, we observed a reduction in *Flk1* transcripts when *Spry4* was overexpressed in transgenic embryos, but also observed a strong effect on the expression of other endothelial markers such as *Pecam1*. It is also possible that reduction of *Flk1* expression seen in *Foxo1* mutants is a secondary consequence of disrupted arterial specification, rather than a primary driver of this defect.

Dll4 is among the earliest markers of arterial gene expression (Chong et al., 2011; Wythe et al., 2013), but precisely how *Dll4* expression is initiated within the early YS and embryo remains poorly understood. While *Dll4* transcription was suggested to be regulated by 5′ binding of FOXC1, FOXC2 and β-catenin in its proximal promoter (Corada et al., 2010; Hayashi and Kume, 2008; Seo et al., 2006), subsequent *in vivo* analysis showed that this region is not sufficient to mediate expression (Wythe et al., 2013). Additionally, endothelial-specific loss of β-catenin failed to alter *Dll4* expression in mice or to produce arteriovenous patterning

Development (2022) 149, dev200131. doi:10.1242/dev.200131

defects (Wythe et al., 2013). Furthermore, functional enhancers were found within intron 3 and upstream at −12 and −16 kb that recapitulated the pattern of endogenous *Dll4* expression (Sacilotto et al., 2013; Wythe et al., 2013), and these regions lacked conserved FOXC1- and FOXC2-binding sites, as well as TCF- and LEF-binding sites. In these current studies, we used a nuclear localized LacZ reporter that recapitulates the normal expression pattern of *Dll4* (Herman et al., 2018). The data presented here clearly show that *Foxo1* is required to sustain *Dll4* and arterial gene expression through the repression of *Spry 2* and *Spry4*, but there are likely other mechanisms involved in activation of *Dll4* and arterial gene expression.

Our data clearly showed that the reduction in *Dll4* expression was far more severe in the *Foxo1*^{ECKO} or null YS than within the embryo proper. In addition to *Dll4*, reduced *Flk1* expression (Fig. S2A) and alterations to *Spry 2* and *Spry4* expression (Fig. S5A) also appeared to be confined to the YS. Similarly, *Spry4* overexpression throughout the embryo and YS using an endothelial-specific *Flk1* promoter (Kappel et al., 1999; Rönicke et al., 1996; Fraser et al., 2005) indicated that *Spry4* overexpression did not alter arterial gene expression in the embryo, but suppressed arterial transcripts (and altered some venous marker expression) in the YS. The mechanism that explains the differential activity of FOXO1, SPRY2 and SPRY4 within the vasculature of the YS versus the embryo proper remains unclear. Future experiments will be required to address numerous possible explanations, including differences in mesodermal cell lineages, differential binding to co-factors and/or differences in post-translational modifications regulated by local cell-cell signaling.

One unresolved issue from these studies is the relationship between abnormal arteriovenous specification and failed vessel remodeling. Both arteriovenous identity and vessel remodeling are regulated by hemodynamic forces, and AV specification relies on pathways that respond to VEGF signaling (Fish and Wythe, 2015; Covassin et al., 2006; Weinstein and Lawson, 2002; Fang et al., 2017). In *Foxo1*^{ECKO}, we detected downregulation of VEGFR2. VEGFR2 and other VEGF receptors have been shown to act as shear stress mechanosensors, signaling through downstream pathways such as the MEK-ERK kinase cascade in response to changes in blood flow (Tzima et al., 2005; Baeyens and Schwartz, 2016). Thus, the downregulation of VEGFR2 in *Foxo1* mutant embryos could prevent ECs from responding to normal blood flow signaling needed for vessel remodeling. Previously, our lab showed that ECs within the vitelline arteries, but not the vitelline veins, migrate directionally in response to hemodynamic changes in YS vasculature (Udan et al., 2013) so it is possible that the loss of FOXO1 and/or the overexpression of *Spry2* and *Spry4* interferes not only with initial *Dll4* specification, but with the ability of the cell to sense mechanical signaling that is necessary to direct cell migration required for remodeling. Further work will be needed to better understand the mechanisms leading both to early *Dll4* expression and those that regulate the cellular responses needed for vessels to adapt to changes in blood flow.

MATERIALS AND METHODS

Animals and genotyping

All animal experiments were conducted according to protocols approved by the Institutional Animal Care and Use Committee of Baylor College of Medicine. *Ella-Cre* and *Tie2-Cre* transgenic mice were purchased from Jackson Labs (003724 and 008863, respectively). *ε-globin-KGFP* mice (Dyer et al., 2001), *Foxo1*$^{flox/flox}$ mice (Paik et al., 2007) and *Dll4-BAC-nLacZ* mice (Herman et al., 2018) were maintained and genotyped as previously described. *Foxo1* germline knockout mice were generated by crossing the *Foxo1*$^{flox/flox}$ mice to *Ella-Cre* mice (Lakso et al., 1996). *Flk1-H2B::YFP* reporter mice were kindly provided by Dr K. Hadjantonakis (Memorial Sloan Kettering Cancer Center, NY, USA) (Fraser et al., 2005).

Immunostaining of whole or sectioned YSs

E8.25 YSs were fixed in 4% PFA, rinsed in PBS, permeabilized with 0.1% TritonX-100 for 1 h and blocked in 2% normal donkey serum/1% BSA for 5 h. YSs were then incubated with anti-PECAM1 antibody (BD Pharmingen, #550274; 1:100) overnight at 4°C. After several PBS washes, YSs were incubated with goat anti-rabbit antibody (Molecular Probes, AlexaFluor 633, 1:500) and DAPI (1:500) overnight at 4°C. Finally, YSs were rinsed in PBS and imaged using the Zeiss LSM510 META confocal microscope. Dissected YSs were cryosectioned at 20 µm and sections were permeabilized and blocked, and incubated with antibodies to caspase 3 (Cell Signaling, 9661, 1:50); connexin 37 (ThermoFisher Scientific, 404200, 1:50), connexin 40 (ThermoFisher Scientific, 364900, 1:50), eNOS (Santa Cruz, sc-654, 1:50), FLK1 (Sigma, V1014, 1:100) or pHistone H3 (Millipore, 06-570, 1:50) overnight at 4°C. The secondary antibody incubation and image acquisition were performed as described previously.

LacZ staining

Dll4-BAC-nLacZ transgenic reporter were examined on *Foxo1* germline or *Foxo1*^{ECKO} (*Tie2-Cre*$^{+/tg}$;*Foxo1*^{floxfloxl}) backgrounds. E8.5 and E9.5 embryos were dissected in ice-cold PBS and fixed in 4% PFA. Embryos were then washed in X-gal rinse buffer (0.02% NP40 and 0.01% sodium deoxycholate; four times for 15 min) and thereafter stained in X-gal solution [5 mM $K_3Fe(CN)_6$, 5 mM $K_4Fe(CN)_6$, 0.01% sodium deoxycholate, 0.02% NP40, 2 mM $MgCl_2$, 5 mM EGTA and 1 mg/ml X-gal] at 37°C overnight. Embryos were then post-fixed in 4% PFA and then cleared in 50% and 70% glycerol. Embryos from the same litter were processed and stained in a 20 ml scintillation vial. Stained embryos were photographed using the Axio ZoomV16 (Zeiss) stereo microscope and thereafter genotyped.

Protein isolation and western blotting

Yolk sacs from three E8.25 wild-type or *Foxo1*^{ECKO} embryos were pooled and lysed in RIPA buffer [10 mM Tris-HCl (pH 8), 1 mM EDTA, 1% Triton X-100, 0.1% sodium deoxycholate, 0.1% SDS, 140 mM NaCl and 1 mM PMSF] supplemented with protease inhibitors. Protein lysates were quantitated using Bradford assay. Twenty micrograms of lysates were electrophoresed on 4-15% protein gels (BioRad), transferred to a PVDF membrane and immunoblotted with antibodies to either FOXO1 or GAPDH (Cell Signaling Technology, 2880 and 97166; 1:2000) overnight at 4°C. After incubation with HRP-conjugated secondary antibodies (Thermo Fisher, 65-6120, 1:5000) for 1 h at room temperature, protein bands were detected via chemiluminescence with Clarity ECL western substrate (BioRad) on film. Western bands were quantified using Fiji gel analyzer and FOXO1 was normalized to GAPDH.

Quantification of *Flk1-H2B::YFP*$^{+}$ cell density, proliferation index and apoptotic index in whole-mount YSs

Acquired wild-type and *Foxo1*^{ECKO} YS whole-mount images (n>3 YSs per genotype, n>3 regions of interest per YS) were made into maximum intensity projections and separated into individual RGB images: red (pHistone-H3/Caspase 3), green (*Flk1-H2B::YFP*) and blue (DAPI). Individual nuclei for RGB channels were segmented and quantified using FARSIGHT. FARSIGHT is an open source image analysis tool box for segmentation and quantitation of biological features courtesy of Badri Roysam (University of Houston, TX, USA; PMID: 18294697; https://github.com/RoysamLab/Farsight-toolkit). We used this to generate both intensity and volume thresholds to distinguish two nuclei as separate. YFP^{+} cell density was defined as the ratio of YFP^{+} nuclei to DAPI^{+} nuclei within that same field of view. Proliferative/apoptotic index was defined as the ratio of PH3^{+}/caspase 3^{+} nuclei to the number of DAPI^{+} nuclei. EC proliferative/apoptotic index was defined as the ratio of YFP^{+};PH3^{+}/caspase 3^{+}

Development (2022) 149, dev200131. doi:10.1242/dev.200131

double-positive nuclei to the number of YFP$^+$ nuclei. The ratios were then averaged over the various wild-type and *Foxo1*^{ECKO} YS images.

Live imaging and analysis of blood flow in *Foxo1* conditional knockout embryos

The *ε-globin-KGFP* reporter expressing GFP in primitive erythroblasts was examined in control and *Foxo1*^{ECKO} background, and litters were dissected at E8.5 or E9.5 for blood velocity analysis. Embryos were dissected under a heated (37°C) dissection stage with warm dissection media (DMEM/F-12, 10% FBS, 100 U/ml penicillin and 100 µg/ml streptomycin). Embryos with an intact ectoplacental cone were placed in a glass-bottomed culture chamber with culture medium (1:1 DMEM/F-12: rat serum, 100 U/ml penicillin and 100 µg/ml streptomycin) and allowed to recover in a 37°C incubator for 20 min. Embryos were then placed on a heated confocal microscope stage (37°C) and imaged using the Zeiss LSM 5 LIVE laser scanning confocal microscope, using the Achroplan 20×/0.45 NA objective. A 200-frame time lapse (in a 512×512 pixel frame) was acquired at 30-50 frames per second. Blood flow time lapse images were acquired at three different locations throughout the YS per embryo, and at least three embryos of each genotype were used for data collection. Individual blood cell velocities in each track were determined from time-lapse movies using Imaris. Individual blood cell velocities from three different locations per embryo were averaged. Average heart beats per minute were calculated by measuring the average time interval between peak velocities during the course of five cardiac cycles in individual velocity profiles for each embryo imaged. Embryos were genotyped after imaging, and blood velocities and heart beats per minute were averaged in wild type and *Foxo1*^{ECKO}.

Magnetic-activated cell sorting of YS ECs

To isolate E8.25 YS ECs, fresh YSs were dissected in ice-cold DMEM/F12 media without Phenol Red (ThermoFisher Scientific, 21041025), individually placed in 100 µl of cold TrypsinLE (Fisher Scientific, 12605010) and kept on ice until all YSs were harvested. Embryos were used for genotyping. To dissociate YSs into a single cell suspension, they were gently triturated with a p200 pipette and incubated on ice for 5 min. This was repeated four times. To inhibit the enzyme, 1 ml of stop solution media and 10% FBS (ThermoFisher Scientific, 26140079) was added. The YS cell suspensions were pelleted at 800 ***g*** for 5 min at 4°C. The pellets were resuspended in 90 µl of cell suspension buffer (PBS, 2% FBS and 2 mM EDTA). 10 µl of CD31 MicroBeads (Miltenyi Biotec, 130-097-418) was added to each YS cell suspension and samples were incubated on ice for 15 min in the dark. Cell mixtures were pelleted at 800 ***g*** for 5 min at 4°C and washed with 1 ml of cell suspension buffer. Cell mixtures were once again pelleted at 800 ***g*** for 5 min at 4°C and resuspended in 200 µl of cell suspension buffer. Cell mixtures were passed through 40 µm cell strainers (Fisher Scientific, 352340) into FACS tubes and strainers were washed with 300 µl of cell suspension buffer. MS columns (Miltenyi Biotec, 130-041-301) were placed on OctoMACS separator and prepared according to the manufacturer's instructions. Cell mixtures were individually passed through columns and the flow through was reapplied through columns to maximize EC retention (CD31$^+$ population). Columns were washed three times with 500 µl cell suspension buffer and all flow through was collected (CD31$^-$ population). Bound cells were released from the columns by removal from magnetic separator. 1 ml of cell suspension buffer was applied to the columns and cells were flushed using a plunger into a 1.5 ml Eppendorf tube. Collected cells were then pelleted at 800 ***g*** for 5 min at 4°C and resuspended in Trizol (Thermo Fisher, 15596018). After genotyping, CD31$^+$ and CD31$^-$ populations from two YSs were combined and processed for RNA isolation (QIAGEN RNeasy Micro Kit, 74004), cDNA synthesis and qRT-qPCR as described below.

RNA isolation and qRT-PCR analysis

Total RNA was isolated from pooled (2-8 YS/sample) E8.25 YSs dissected from either *Tie2-Cre*$^{+/tg}$*; Foxo1*$^{+/flox}$ or *Tie2-Cre*$^{+/tg}$*; Foxo1*$^{flox/flox}$ embryos. Purified RNA was reverse transcribed (ThermoFisher Scientific, 11752-050) and gene expression analysis was performed using TaqMan real-time assays for *Foxo1*, *Adm*, *Bmper*, *Vcam1* and a panel of endothelial, arterial and venous markers (see Table S2 for list). The data were normalized to *Gapdh* (Pfaffl, 2001) and relative expression ratios between control and *Foxo1*^{ECKO} embryos were determined. Endogenous *Foxo1*, *Spry1*, *Spry2*, *Spry3* and *Spry4* expression from pooled E8.25 YSs (CD1 strain) was also probed by TaqMan real-time assay, but expression was calculated as fold change relative to *Foxo1*.

Endogenous *Dll4* expression was measured in either germline *Foxo1* knockouts or *Foxo1*^{ECKO} embryos at E8.25. The allantois was used for genotyping and total RNA was extracted from individual embryos and YSs (n≥3) and probed for *Dll4* expression using a TaqMan assay to measure fold change of expression between controls and homozygous *Foxo1*^{ECKO} mutants. An unpaired Student's *t*-test was used to assess statistical significance and P<0.05 was considered statistically significant.

Chromatin immunoprecipitation (ChIP) and qPCR

To determine endogenous FOXO1 chromatin occupancy, E8.25 YSs from CD1 embryos were used for chromatin extraction. Freshly dissected YSs were dissociated in ice cold PBS with protease inhibitors and the tissue was then crosslinked with 1.5% formaldehyde, followed by incubation with 125 mM glycine and washed with PBS. After centrifugation, the pellet was resuspended in cell lysis buffer [5 mM PIPES (pH 8), 85 mM KCl and 0.5% NP40]. The samples were spun and the pellet was resuspended in nuclear lysis buffer [50 mM Tris-HCl (pH 8.1), 10 mM EDTA; 1% SDS] and then sonicated on ice using a Bioruptor (Diagenode) to obtain sheared chromatin ranging between 100 and 500 bp. ChIP was performed according to the instructions for Magna ChIP kit (Millipore, 17-10085) using 5 µg of anti-FOXO1 antibody (Abcam, ab39670) or rabbit IgG (Millipore, 12370). The crosslinks were then reversed, and the purified DNA was then analyzed by qPCR in technical triplicates using SYBR green master mix and the primers listed in Table S1 to measure the percentage of co-precipitating DNA relative to input (% input) in *Spry2* and *Spry4* genomic regions.

Cloning of murine *Spry2* and *Spry4* promoter constructs and luciferase assay

Genomic regions of ∼2 kb in length of murine *Spry2* and *Spry4* were PCR amplified using primers listed in Table S1 and using BAC clones of C57BL6 genomic DNA as template DNA (CH29-611D15 and CH29-100M12, respectively; CHORI BAC/PAC resources). PCR fragments were ligated into pCRII-TOPO vector, sequenced and then subcloned into pGL3-Promoter vector (Promega). H1299 cells (ATCC, CRL-5803) were maintained in DMEM media supplemented with 10% FBS, 100 U/ml penicillin and 100 µg/ml streptomycin. For transient transfections, 50,000 cells were plated (48-well plate) and after 24 h, each well was co-transfected with 200 ng of *Spry2* and *Spry4* promoter construct, 10 ng of pRL-TK and 125 ng expression plasmid (pcDNA3-FOXO::FLAG; Addgene 13507) using manufacturer's recommendations for lipofectamine 3000. The total amount of expression plasmid transfected per well was kept constant with varying amounts of pcDNA3.1 vector. As a negative control, a *Foxo1* plasmid encoding a deleted DNA-binding domain (amino acids 208-220) was used (Addgene 10694). After 24 h, cells were lysed and analyzed for firefly and *Renilla* luciferase activities according to the procedure outlined in the Dual-Glo luciferase assay system (Promega, E2920). All luciferase assays were performed in triplicate and repeated at least three times. An unpaired Student's *t*-test was used to assess statistical significance (P<0.05 was considered statistically significant) and the averages and standard deviation from triplicate samples from representative assays were shown.

Transient endothelial-specific *Sprouty* expression in embryos

A mouse *Spry4* cDNA clone (TransOmics clone BC057005) was used as a template to PCR amplify the coding sequence with 5′ *Sac*I and 3′ *Pme*I restriction sites (5′ GAGCTCCCAGCCTCATGGAGCCC 3′ and 5′ GTTTAAACTCAGAAAGGCTTGTCAGAC 3′), and subcloned into pCRIITOPO vector (S4-2). The internal ribosome entry site (IRES) sequence was amplified from pIRES-hrGFP1a vector (Agilent Technologies) with 5′ EcoRV and 3′ EcoRI restriction sites using primers 5′ CT-ATAGATATCACCCCCCTCTCCCTA 3′ and 5′ GCATGAATTCGGTT-GTGGCCATTATCATCGTG 3′ and subcloned into pCRIITOPO vector

(IRES-4). To assemble the final transgenic construct, clones S4-2 and IRES-4 were excised with 5′ *Ecl136*II and 3′ NotI, and 5′ NotI and 3′ Ecl136II, respectively, and co-ligated into *Flk1*-H2B/EYFP vector (kindly provided by Dr K. Hadjantonakis, Memorial Sloan Kettering Cancer Center, NY, USA) via a blunt-ended HindIII site. The *Flk1*-H2B/EYFP vector has a well characterized *Flk1* promoter and intronic enhancer sequences that drive YFP expression in ECs (Fraser et al., 2005). All clones were verified by DNA sequencing and the final transgenic construct was excised with 5′ SalI and 3′ XbaI to purify a 4.5 kb fragment for pronuclear microinjection, which was performed at the BCM Genetically Engineered Mouse Core. Transient transgenic embryos were dissected with the YS intact and initially screened for YFP expression using confocal microscopy. Gross morphology of the embryo and YS vasculature was examined at E9.5 while arterial marker analysis (connexin 37, connexin 40, *Dll4*, *Efnb2* and *Hey1*) was performed at E8.25. Embryos and YSs were individually lysed in Trizol for RNA extraction and screened for YFP-positive and -negative samples (n=3 each) that were stage matched at 4-7 somites (Fig. S7A). Additionally, the ratio of exogenous over endogenous murine *Spry4* expression was quantitated for YFP-positive samples using transcript-specific primers (Fig. S7B). Detection was via the Sybr-green or Taqman assay (for arterial markers) and fold change of expression between YFP-positive and -negative samples, and statistical analysis were performed as previously described.

Acknowledgements
We thank Tegy J. Vadakkan in the Optical imaging and vital microscopy core facility.

Competing interests
The authors declare no competing or financial interests.

Author contributions
Conceptualization: N.L.-V., R.L.Y.W., M.D.G., R.A.P., T.L.R., J.D.W., M.E.D.; Methodology: A.M.R.; Validation: N.L.-V.; Data curation: N.L.-V., R.L.Y.W., M.D.G., R.S.U., T.L.R., A.M.R.; Writing - original draft: N.L.-V., R.L.Y.W.; Writing - review & editing: N.L.-V., R.L.Y.W., M.D.G., R.S.U., R.A.P., T.L.R., J.D.W., M.E.D.; Supervision: M.E.D.; Funding acquisition: M.E.D.

Funding
The authors' research was funded by the National Institutes of Health (R01 HD099026). Open access funding provided by the National Institutes of Health. Deposited in PMC for immediate release.

Peer review history
The peer review history is available online at https://journals.biologists.com/dev/article-lookup/doi/10.1242/dev.200131.

References
Adams, R. H., Wilkinson, G. A., Weiss, C., Diella, F., Gale, N. W., Deutsch, U., Risau, W. and Klein, R. (1999). Roles of ephrinB ligands and EphB receptors in cardiovascular development: demarcation of arterial/venous domains, vascular morphogenesis, and sprouting angiogenesis. *Genes Dev.* **13**, 295-306. doi:10.1101/gad.13.3.295

Aitsebaomo, J., Portbury, A. L., Schisler, J. C. and Patterson, C. (2008). Brothers and sisters: molecular insights into arterial-venous heterogeneity. *Circ. Res.* **103**, 929-939. doi:10.1161/CIRCRESAHA.108.184937

Albert, P. S., Brown, S. J. and Riddle, D. L. (1981). Sensory control of dauer larva formation in Caenorhabditis elegans. *J. Comp. Neurol.* **198**, 435-451. doi:10.1002/cne.901980305

Baeyens, N. and Schwartz, M. A. (2016). Biomechanics of vascular mechanosensation and remodeling. *Mol. Biol. Cell* **27**, 7-11. doi:10.1091/mbc.E14-11-1522

Beard, R. S., Jr, Hoettels, B. A., Meegan, J. E., Wertz, T. S., Cha, B. J., Yang, X., Oxford, J. T., Wu, M. H. and Yuan, S. Y. (2020). AKT2 maintains brain endothelial claudin-5 expression and selective activation of IR/AKT2/FOXO1-signaling reverses barrier dysfunction. *J. Cereb. Blood Flow Metab.* **40**, 374-391. doi:10.1177/0271678X18817512

Bernatchez, P. N., Soker, S. and Sirois, M. G. (1999). Vascular endothelial growth factor effect on endothelial cell proliferation, migration, and platelet-activating factor synthesis is Flk-1-dependent. *J. Biol. Chem.* **274**, 31047-31054. doi:10.1074/jbc.274.43.31047

Casci, T., Vinos, J. and Freeman, M. (1999). Sprouty, an intracellular inhibitor of Ras signaling. *Cell* **96**, 655-665. doi:10.1016/S0092-8674(00)80576-0

Chlench, S., Mecha Disassa, N., Hohberg, M., Hoffmann, C., Pohlkamp, T., Beyer, G., Bongrazio, M., da Silva-Azevedo, L., Baum, O., Pries, A. R. et al. (2007). Regulation of Foxo-1 and the angiopoietin-2/Tie2 system by shear stress. *FEBS Lett.* **581**, 673-680. doi:10.1016/j.febslet.2007.01.028

Chong, D. C., Koo, Y., Xu, K., Fu, S. and Cleaver, O. (2011). Stepwise arteriovenous fate acquisition during mammalian vasculogenesis. *Dev. Dyn.* **240**, 2153-2165. doi:10.1002/dvdy.22706

Chu, M., Li, T., Shen, B., Cao, X., Zhong, H., Zhang, L., Zhou, F., Ma, W., Jiang, H., Xie, P. et al. (2016). Angiopoietin receptor Tie2 is required for vein specification and maintenance via regulating COUP-TFII. *eLife* **5**, e21032. doi:10.7554/eLife.21032

Cleaver, O. and Krieg, P. A. (1998). VEGF mediates angioblast migration during development of the dorsal aorta in Xenopus. *Development* **125**, 3905-3914. doi:10.1242/dev.125.19.3905

Corada, M., Nyqvist, D., Orsenigo, F., Caprini, A., Giampietro, C., Taketo, M. M., Iruela-Arispe, M. L., Adams, R. H. and Dejana, E. (2010). The Wnt/β-catenin pathway modulates vascular remodeling and specification by upregulating Dll4/Notch signaling. *Dev. Cell* **18**, 938-949. doi:10.1016/j.devcel.2010.05.006

Covassin, L. D., Villefranc, J. A., Kacergis, M. C., Weinstein, B. M. and Lawson, N. D. (2006). Distinct genetic interactions between multiple Vegf receptors are required for development of different blood vessel types in zebrafish. *Proc. Natl. Acad. Sci. USA* **103**, 6554-6559. doi:10.1073/pnas.0506886103

Dang, L. T. H., Aburatani, T., Marsh, G. A., Johnson, B. G., Alimperti, S., Yoon, C. J., Huang, A., Szak, S., Nakagawa, N., Gomez, I. et al. (2017). Hyperactive FOXO1 results in lack of tip stalk identity and deficient microvascular regeneration during kidney injury. *Biomaterials* **141**, 314-329. doi:10.1016/j.biomaterials.2017.07.010

Dharaneeswaran, H., Abid, M. R., Yuan, L., Dupuis, D., Beeler, D., Spokes, K. C., Janes, L., Sciuto, T., Kang, P. M., Jaminet, S.-C. S. et al. (2014). FOXO1-mediated activation of Akt plays a critical role in vascular homeostasis. *Circ. Res.* **115**, 238-251. doi:10.1161/CIRCRESAHA.115.303227

Dickinson, M. E., Flenniken, A. M., Ji, X., Teboul, L., Wong, M. D., White, J. K., Meehan, T. F., Weninger, W. J., Westerberg, H., Adissu, H. et al. (2016). High-throughput discovery of novel developmental phenotypes. *Nature* **537**, 508-514. doi:10.1038/nature19356

Dixit, M., Bess, E., Fisslthaler, B., Hartel, F. V., Noll, T., Busse, R. and Fleming, I. (2008). Shear stress-induced activation of the AMP-activated protein kinase regulates FoxO1a and angiopoietin-2 in endothelial cells. *Cardiovasc. Res.* **77**, 160-168. doi:10.1093/cvr/cvm017

Duarte, A., Hirashima, M., Benedito, R., Trindade, A., Diniz, P., Bekman, E., Costa, L., Henrique, D. and Rossant, J. (2004). Dosage-sensitive requirement for mouse Dll4 in artery development. *Genes Dev.* **18**, 2474-2478. doi:10.1101/gad.1239004

Dyer, M. A., Farrington, S. M., Mohn, D., Munday, J. R. and Baron, M. H. (2001). Indian hedgehog activates hematopoiesis and vasculogenesis and can respecify prospective neurectodermal cell fate in the mouse embryo. *Development* **128**, 1717-1730. doi:10.1242/dev.128.10.1717

Dziadek, M. and Adamson, E. (1978). Localization and synthesis of alphafoetoprotein in post-implantation mouse embryos. *J. Embryol. Exp. Morphol.* **43**, 289-313. doi:10.1242/dev.43.1.289

Eklund, L. and Olsen, B. R. (2006). Tie receptors and their angiopoietin ligands are context-dependent regulators of vascular remodeling. *Exp. Cell Res.* **312**, 630-641. doi:10.1016/j.yexcr.2005.09.002

Fang, J. S., Coon, B. G., Gillis, N., Chen, Z., Qiu, J., Chittenden, T. W., Burt, J. M., Schwartz, M. A. and Hirschi, K. K. (2017). Shear-induced Notch-Cx37-p27 axis arrests endothelial cell cycle to enable arterial specification. *Nat. Commun.* **8**, 2149. doi:10.1038/s41467-017-01742-7

Ferdous, A., Morris, J., Abedin, M. J., Collins, S., Richardson, J. A. and Hill, J. A. (2011). Forkhead factor FoxO1 is essential for placental morphogenesis in the developing embryo. *Proc. Natl. Acad. Sci. USA* **108**, 16307-16312. doi:10.1073/pnas.1107341108

Fischer, A., Schumacher, N., Maier, M., Sendtner, M. and Gessler, M. (2004). The Notch target genes Hey1 and Hey2 are required for embryonic vascular development. *Genes Dev.* **18**, 901-911. doi:10.1101/gad.291004

Fish, J. E. and Wythe, J. D. (2015). The molecular regulation of arteriovenous specification and maintenance. *Dev. Dyn.* **244**, 391-409. doi:10.1002/dvdy.24252

Fish, J. E., Cantu Gutierrez, M., Dang, L. T., Khyzha, N., Chen, Z., Veitch, S., Cheng, H. S., Khor, M., Antounians, L., Njock, M.-S. et al. (2017). Dynamic regulation of VEGF-inducible genes by an ERK/ERG/p300 transcriptional network. *Development* **144**, 2428-2444. doi:10.1242/dev.146050

Fosbrink, M., Niculescu, F., Rus, V., Shin, M. L. and Rus, H. (2006). C5b-9-induced endothelial cell proliferation and migration are dependent on Akt inactivation of forkhead transcription factor FOXO1. *J. Biol. Chem.* **281**, 19009-19018. doi:10.1074/jbc.M602055200

Fraser, S. T., Hadjantonakis, A.-K., Sahr, K. E., Willey, S., Kelly, O. G., Jones, E. A., Dickinson, M. E. and Baron, M. H. (2005). Using a histone yellow fluorescent protein fusion for tagging and tracking endothelial cells in ES cells and mice. *Genesis* **42**, 162-171. doi:10.1002/gene.20139

Fukumoto, M., Kondo, K., Uni, K., Ishiguro, T., Hayashi, M., Ueda, S., Mori, I., Niimi, K., Tashiro, F., Miyazaki, S. et al. (2018). Tip-cell behavior is regulated by transcription factor FoxO1 under hypoxic conditions in developing mouse retinas. *Angiogenesis* **21**, 203-214. doi:10.1007/s10456-017-9588-z

Furuyama, T., Kitayama, K., Shimoda, Y., Ogawa, M., Sone, K., Yoshida-Araki, K., Hisatsune, H., Nishikawa, S., Nakayama, K., Nakayama, K. et al. (2004). Abnormal angiogenesis in Foxo1 (Fkhr)-deficient mice. *J. Biol. Chem.* **279**, 34741-34749. doi:10.1074/jbc.M314214200

Gale, N. W., Dominguez, M. G., Noguera, I., Pan, L., Hughes, V., Valenzuela, D. M., Murphy, A. J., Adams, N. C., Lin, H. C., Holash, J. et al. (2004). Haploinsufficiency of delta-like 4 ligand results in embryonic lethality due to major defects in arterial and vascular development. *Proc. Natl. Acad. Sci. USA* **101**, 15949-15954. doi:10.1073/pnas.0407290101

Goetz, J. G., Steed, E., Ferreira, R. R., Roth, S., Ramspacher, C., Boselli, F., Charvin, G., Liebling, M., Wyart, C., Schwab, Y. et al. (2014). Endothelial cilia mediate low flow sensing during zebrafish vascular development. *Cell Rep* **6**, 799-808. doi:10.1016/j.celrep.2014.01.032

Gong, Y., Yang, X., He, Q., Gower, L., Prudovsky, I., Vary, C. P. H., Brooks, P. C. and Friesel, R. E. (2013). Sprouty4 regulates endothelial cell migration via modulating integrin beta3 stability through c-Src. *Angiogenesis* **16**, 861-875. doi:10.1007/s10456-013-9361-x

Gridley, T. (2010). Notch signaling in the vasculature. *Curr. Top. Dev. Biol.* **92**, 277-309. doi:10.1016/S0070-2153(10)92009-7

Hayashi, H. and Kume, T. (2008). Foxc transcription factors directly regulate Dll4 and Hey2 expression by interacting with the VEGF-Notch signaling pathways in endothelial cells. *PLoS ONE* **3**, e2401. doi:10.1371/journal.pone.0002401

Herman, A. M., Rhyner, A. M., Devine, W. P., Marrelli, S. P., Bruneau, B. G. and Wythe, J. D. (2018). A novel reporter allele for monitoring Dll4 expression within the embryonic and adult mouse. *Biol. Open* **7**, bio026799. doi:10.1242/bio.026799

Herzog, Y., Guttmann-Raviv, N. and Neufeld, G. (2005). Segregation of arterial and venous markers in subpopulations of blood islands before vessel formation. *Dev. Dyn.* **232**, 1047-1055. doi:10.1002/dvdy.20257

Hosaka, T., Biggs, W. H., III, Tieu, D., Boyer, A. D., Varki, N. M., Cavenee, W. K. and Arden, K. C. (2004). Disruption of forkhead transcription factor (FOXO) family members in mice reveals their functional diversification. *Proc. Natl. Acad. Sci. USA* **101**, 2975-2980. doi:10.1073/pnas.0400093101

Huang, H. and Tindall, D. J. (2007). Dynamic FoxO transcription factors. *J. Cell Sci.* **120**, 2479-2487. doi:10.1242/jcs.001222

Hwa, J. J., Beckouche, N., Huang, L., Kram, Y., Lindskog, H. and Wang, R. A. (2017). Abnormal arterial-venous fusions and fate specification in mouse embryos lacking blood flow. *Sci. Rep.* **7**, 11965. doi:10.1038/s41598-017-12353-z

Ji, R. P., Phoon, C. K., Aristizabal, O., Mcgrath, K. E., Palis, J. and Turnbull, D. H. (2003). Onset of cardiac function during early mouse embryogenesis coincides with entry of primitive erythroblasts into the embryo proper. *Circ. Res.* **92**, 133-135. doi:10.1161/01.RES.0000056532.18710.C0

Jiang, Z., Tian, J., Zhang, W., Yan, H., Liu, L., Huang, Z., Lou, J. and Ma, X. (2017). Forkhead protein FoxO1 acts as a repressor to inhibit cell differentiation in human fetal pancreatic progenitor cells. *J. Diabetes Res.* **2017**, 6726901. doi:10.1155/2017/6726901

Jiramongkol, Y. and Lam, E. W.-F. (2020). FOXO transcription factor family in cancer and metastasis. *Cancer Metastasis Rev.* **39**, 681-709. doi:10.1007/s10555-020-09883-w

Jones, E. A. V., Baron, M. H., Fraser, S. E. and Dickinson, M. E. (2004). Measuring hemodynamic changes during mammalian development. *Am. J. Physiol. Heart Circ. Physiol.* **287**, H1561-H1569. doi:10.1152/ajpheart.00081.2004

Kappel, A., Rönicke, V., Damert, A., Flamme, I., Risau, W. and Breier, G. (1999). Identification of vascular endothelial growth factor (VEGF) receptor-2 (Flk-1) promoter/enhancer sequences sufficient for angioblast and endothelial cell-specific transcription in transgenic mice. *Blood* **93**, 4284-4292. doi:10.1182/blood.V93.12.4284

Kim, Y. H., Choi, J., Yang, M. J., Hong, S. P., Lee, C.-K., Kubota, Y., Lim, D.-S. and Koh, G. Y. (2019). A MST1-FOXO1 cascade establishes endothelial tip cell polarity and facilitates sprouting angiogenesis. *Nat. Commun.* **10**, 838. doi:10.1038/s41467-019-08773-2

Kisanuki, Y. Y., Hammer, R. E., Miyazaki, J.-I., Williams, S. C., Richardson, J. A. and Yanagisawa, M. (2001). Tie2-Cre transgenic mice: a new model for endothelial cell-lineage analysis in vivo. *Dev. Biol.* **230**, 230-242. doi:10.1006/dbio.2000.0106

Kondrychyn, I., Kelly, D. J., Carretero, N. T., Nomori, A., Kato, K., Chong, J., Nakajima, H., Okuda, S., Mochizuki, N. and Phng, L.-K. (2020). Marcksl1 modulates endothelial cell mechanoresponse to haemodynamic forces to control blood vessel shape and size. *Nat. Commun.* **11**, 5476. doi:10.1038/s41467-020-19308-5

Krebs, L. T., Xue, Y., Norton, C. R., Shutter, J. R., Maguire, M., Sundberg, J. P., Gallahan, D., Closson, V., Kitajewski, J., Callahan, R. et al. (2000). Notch signaling is essential for vascular morphogenesis in mice. *Genes Dev.* **14**, 1343-1352. doi:10.1101/gad.14.11.1343

Krebs, L. T., Starling, C., Chervonsky, A. V. and Gridley, T. (2010). Notch1 activation in mice causes arteriovenous malformations phenocopied by ephrinB2 and EphB4 mutants. *Genesis* **48**, 146-150. doi:10.1002/dvg.20599

Lakso, M., Pichel, J. G., Gorman, J. R., Sauer, B., Okamoto, Y., Lee, E., Alt, F. W. and Westphal, H. (1996). Efficient in vivo manipulation of mouse genomic sequences at the zygote stage. *Proc. Natl. Acad. Sci. USA* **93**, 5860-5865. doi:10.1073/pnas.93.12.5860

Langlet, F., Haeusler, R. A., Lindén, D., Ericson, E., Norris, T., Johansson, A., Cook, J. R., Aizawa, K., Wang, L., Buettner, C. et al. (2017). Selective inhibition of FOXO1 activator/repressor balance modulates hepatic glucose handling. *Cell* **171**, 824-835.e18. doi:10.1016/j.cell.2017.09.045

Lawson, N. D., Scheer, N., Pham, V. N., Kim, C.-H., Chitnis, A. B., Campos-Ortega, J. A. and Weinstein, B. M. (2001). Notch signaling is required for arterial-venous differentiation during embryonic vascular development. *Development* **128**, 3675-3683. doi:10.1242/dev.128.19.3675

Lawson, N. D., Vogel, A. M. and Weinstein, B. M. (2002). sonic hedgehog and vascular endothelial growth factor act upstream of the Notch pathway during arterial endothelial differentiation. *Dev. Cell* **3**, 127-136. doi:10.1016/S1534-5807(02)00198-3

le Noble, F., Moyon, D., Pardanaud, L., Yuan, L., Djonov, V., Matthijsen, R., Bréant, C., Fleury, V. and Eichmann, A. (2004). Flow regulates arterial-venous differentiation in the chick embryo yolk sac. *Development* **131**, 361-375. doi:10.1242/dev.00929

le Noble, F., Fleury, V., Pries, A., Corvol, P., Eichmann, A. and Reneman, R. S. (2005). Control of arterial branching morphogenesis in embryogenesis: go with the flow. *Cardiovasc. Res.* **65**, 619-628. doi:10.1016/j.cardiores.2004.09.018

Lee, S. H., Schloss, D. J., Jarvis, L., Krasnow, M. A. and Swain, J. L. (2001). Inhibition of angiogenesis by a mouse sprouty protein. *J. Biol. Chem.* **276**, 4128-4133. doi:10.1074/jbc.M006922200

Liu, Z.-J., Shirakawa, T., Li, Y., Soma, A., Oka, M., Dotto, G. P., Fairman, R. M., Velazquez, O. C. and Herlyn, M. (2003). Regulation of Notch1 and Dll4 by vascular endothelial growth factor in arterial endothelial cells: implications for modulating arteriogenesis and angiogenesis. *Mol. Cell. Biol.* **23**, 14-25. doi:10.1128/MCB.23.1.14-25.2003

Lobov, I. B., Renard, R. A., Papadopoulos, N., Gale, N. W., Thurston, G., Yancopoulos, G. D. and Wiegand, S. J. (2007). Delta-like ligand 4 (Dll4) is induced by VEGF as a negative regulator of angiogenic sprouting. *Proc. Natl. Acad. Sci. USA* **104**, 3219-3224. doi:10.1073/pnas.0611206104

Lucitti, J. L., Jones, E. A. V., Huang, C., Chen, J., Fraser, S. E. and Dickinson, M. E. (2007). Vascular remodeling of the mouse yolk sac requires hemodynamic force. *Development* **134**, 3317-3326. doi:10.1242/dev.02883

Mack, J. J. and Iruela-Arispe, M. L. (2018). NOTCH regulation of the endothelial cell phenotype. *Curr. Opin Hematol.* **25**, 212-218. doi:10.1097/MOH.0000000000000425

Mack, J. J., Mosqueiro, T. S., Archer, B. J., Jones, W. M., Sunshine, H., Faas, G. C., Briot, A., Aragón, R. L., Su, T., Romay, M. C. et al. (2017). NOTCH1 is a mechanosensor in adult arteries. *Nat. Commun.* **8**, 1620. doi:10.1038/s41467-017-01741-8

Mailhos, C., Modlich, U., Lewis, J., Harris, A., Bicknell, R. and Ish-Horowicz, D. (2001). Delta4, an endothelial specific notch ligand expressed at sites of physiological and tumor angiogenesis. *Differentiation* **69**, 135-144. doi:10.1046/j.1432-0436.2001.690207.x

Masumura, T., Yamamoto, K., Shimizu, N., Obi, S. and Ando, J. (2009). Shear stress increases expression of the arterial endothelial marker ephrinB2 in murine ES cells via the VEGF-Notch signaling pathways. *Arterioscler. Thromb. Vasc. Biol.* **29**, 2125-2131. doi:10.1161/ATVBAHA.109.193185

Niimi, K., Ueda, M., Fukumoto, M., Kohara, M., Sawano, T., Tsuchihashi, R., Shibata, S., Inagaki, S. and Furuyama, T. (2017). Transcription factor FOXO1 promotes cell migration toward exogenous ATP via controlling P2Y1 receptor expression in lymphatic endothelial cells. *Biochem. Biophys. Res. Commun.* **489**, 413-419. doi:10.1016/j.bbrc.2017.05.156

Obi, S., Yamamoto, K., Shimizu, N., Kumagaya, S., Masumura, T., Sokabe, T., Asahara, T. and Ando, J. (2009). Fluid shear stress induces arterial differentiation of endothelial progenitor cells. *J. Appl. Physiol. (1985)* **106**, 203-211. doi:10.1152/japplphysiol.00197.2008

Paik, J.-H., Kollipara, R., Chu, G., Ji, H., Xiao, Y., Ding, Z., Miao, L., Tothova, Z., Horner, J. W., Carrasco, D. R. et al. (2007). FoxOs are lineage-restricted redundant tumor suppressors and regulate endothelial cell homeostasis. *Cell* **128**, 309-323. doi:10.1016/j.cell.2006.12.029

Palis, J. (2014). Primitive and definitive erythropoiesis in mammals. *Front. Physiol.* **5**, 3. doi:10.3389/fphys.2014.00003

Pfaffl, M. W. (2001). A new mathematical model for relative quantification in real-time RT-PCR. *Nucleic Acids Res.* **29**, e45. doi:10.1093/nar/29.9.e45

Potente, M., Urbich, C., Sasaki, K.-I., Hofmann, W. K., Heeschen, C., Aicher, A., Kollipara, R., Depinho, R. A., Zeiher, A. M. and Dimmeler, S. (2005). Involvement of Foxo transcription factors in angiogenesis and postnatal neovascularization. *J. Clin. Invest.* **115**, 2382-2392. doi:10.1172/JCI23126

Riddell, M., Nakayama, A., Hikita, T., Mirzapourshafiyi, F., Kawamura, T., Pasha, A., Li, M., Masuzawa, M., Looso, M., Steinbacher, T. et al. (2018). aPKC controls endothelial growth by modulating c-Myc via FoxO1 DNA-binding ability. *Nat. Commun.* **9**, 5357. doi:10.1038/s41467-018-07739-0

Risau, W. (1994). Angiogenesis and endothelial cell function. *Arzneimittelforschung* **44**, 416-417.

Risau, W. and Flamme, I. (1995). Vasculogenesis. *Annu. Rev. Cell Dev. Biol.* **11**, 73-91. doi:10.1146/annurev.cb.11.110195.000445

Rönicke, V., Risau, W. and Breier, G. (1996). Characterization of the endothelium-specific murine vascular endothelial growth factor receptor-2 (Flk-1) promoter. *Circ. Res.* **79**, 277-285. doi:10.1161/01.RES.79.2.277

Rudnicki, M., Abdifarkosh, G., Nwadozi, E., Ramos, S. V., Makki, A., Sepa-Kishi, D. M., Ceddia, R. B., Perry, C. G., Roudier, E. and Haas, T. L. (2018). Endothelial-specific FoxO1 depletion prevents obesity-related disorders by increasing vascular metabolism and growth. *eLife* **7**, e39780. doi:10.7554/eLife.39780

Sacilotto, N., Monteiro, R., Fritzsche, M., Becker, P. W., Sanchez-del-Campo, L., Liu, K., Pinheiro, P., Ratnayaka, I., Davies, B., Goding, C. R. et al. (2013). Analysis of Dll4 regulation reveals a combinatorial role for Sox and Notch in arterial development. *Proc. Natl. Acad. Sci. USA* **110**, 11893-11898. doi:10.1073/pnas.1300805110

Schlaeger, T. M., Bartunkova, S., Lawitts, J. A., Teichmann, G., Risau, W., Deutsch, U. and Sato, T. N. (1997). Uniform vascular-endothelial-cell-specific gene expression in both embryonic and adult transgenic mice. *Proc. Natl. Acad. Sci. USA* **94**, 3058-3063. doi:10.1073/pnas.94.7.3058

Sengupta, A., Chakraborty, S., Paik, J., Yutzey, K. E. and Evans-Anderson, H. J. (2012). FoxO1 is required in endothelial but not myocardial cell lineages during cardiovascular development. *Dev. Dyn.* **241**, 803-813. doi:10.1002/dvdy.23759

Seo, S., Fujita, H., Nakano, A., Kang, M., Duarte, A. and Kume, T. (2006). The forkhead transcription factors, Foxc1 and Foxc2, are required for arterial specification and lymphatic sprouting during vascular development. *Dev. Biol.* **294**, 458-470. doi:10.1016/j.ydbio.2006.03.035

Shay-Salit, A., Shushy, M., Wolfovitz, E., Yahav, H., Breviario, F., Dejana, E. and Resnick, N. (2002). VEGF receptor 2 and the adherens junction as a mechanical transducer in vascular endothelial cells. *Proc. Natl. Acad. Sci. USA* **99**, 9462-9467. doi:10.1073/pnas.142224299

Shutter, J. R., Scully, S., Fan, W., Richards, W. G., Kitajewski, J., Deblandre, G. A., Kintner, C. R. and Stark, K. L. (2000). Dll4, a novel Notch ligand expressed in arterial endothelium. *Genes Dev.* **14**, 1313-1318. doi:10.1101/gad.14.11.1313

Siekmann, A. F. and Lawson, N. D. (2007). Notch signalling limits angiogenic cell behaviour in developing zebrafish arteries. *Nature* **445**, 781-784. doi:10.1038/nature05577

Su, T., Stanley, G., Sinha, R., D'Amato, G., Das, S., Rhee, S., Chang, A. H., Poduri, A., Raftrey, B., Dinh, T. T. et al. (2018). Single-cell analysis of early progenitor cells that build coronary arteries. *Nature* **559**, 356-362. doi:10.1038/s41586-018-0288-7

Sun, X., Chen, W.-D. and Wang, Y.-D. (2017). DAF-16/FOXO transcription factor in aging and longevity. *Front. Pharmacol.* **8**, 548. doi:10.3389/fphar.2017.00548

Swift, M. R. and Weinstein, B. M. (2009). Arterial-venous specification during development. *Circ. Res.* **104**, 576-588. doi:10.1161/CIRCRESAHA.108.188805

Taniguchi, K., Ishizaki, T., Ayada, T., Sugiyama, Y., Wakabayashi, Y., Sekiya, T., Nakagawa, R. and Yoshimura, A. (2009). Sprouty4 deficiency potentiates Ras-independent angiogenic signals and tumor growth. *Cancer Sci.* **100**, 1648-1654. doi:10.1111/j.1349-7006.2009.01214.x

Tzima, E., Irani-Tehrani, M., Kiosses, W. B., Dejana, E., Schultz, D. A., Engelhardt, B., Cao, G., Delisser, H. and Schwartz, M. A. (2005). A mechanosensory complex that mediates the endothelial cell response to fluid shear stress. *Nature* **437**, 426-431. doi:10.1038/nature03952

Udan, R. S., Vadakkan, T. J. and Dickinson, M. E. (2013). Dynamic responses of endothelial cells to changes in blood flow during vascular remodeling of the mouse yolk sac. *Development* **140**, 4041-4050. doi:10.1242/dev.096255

Wang, H. U., Chen, Z.-F. and Anderson, D. J. (1998). Molecular distinction and angiogenic interaction between embryonic arteries and veins revealed by ephrin-B2 and its receptor Eph-B4. *Cell* **93**, 741-753. doi:10.1016/S0092-8674(00)81436-1

Weinstein, B. M. and Lawson, N. D. (2002). Arteries, veins, Notch, and VEGF. *Cold Spring Harb. Symp. Quant. Biol.* **67**, 155-162. doi:10.1101/sqb.2002.67.155

Wietecha, M. S., Chen, L., Ranzer, M. J., Anderson, K., Ying, C., Patel, T. B. and Dipietro, L. A. (2011). Sprouty2 downregulates angiogenesis during mouse skin wound healing. *Am. J. Physiol. Heart Circ. Physiol.* **300**, H459-H467. doi:10.1152/ajpheart.00244.2010

Wilhelm, K., Happel, K., Eelen, G., Schoors, S., Oellerich, M. F., Lim, R., Zimmermann, B., Aspalter, I. M., Franco, C. A., Boettger, T. et al. (2016). FOXO1 couples metabolic activity and growth state in the vascular endothelium. *Nature* **529**, 216-220. doi:10.1038/nature16498

Wragg, J. W., Durant, S., Mcgettrick, H. M., Sample, K. M., Egginton, S. and Bicknell, R. (2014). Shear stress regulated gene expression and angiogenesis in vascular endothelium. *Microcirculation* **21**, 290-300. doi:10.1111/micc.12119

Wythe, J. D., Dang, L. T. H., Devine, W. P., Boudreau, E., Artap, S. T., He, D., Schachterle, W., Stainier, D. Y. R., Oettgen, P., Black, B. L. et al. (2013). ETS factors regulate Vegf-dependent arterial specification. *Dev. Cell* **26**, 45-58. doi:10.1016/j.devcel.2013.06.007

Xue, Y., Gao, X., Lindsell, C. E., Norton, C. R., Chang, B., Hicks, C., Gendron-Maguire, M., Rand, E. B., Weinmaster, G. and Gridley, T. (1999). Embryonic lethality and vascular defects in mice lacking the Notch ligand Jagged1. *Hum. Mol. Genet.* **8**, 723-730. doi:10.1093/hmg/8.5.723

You, L.-R., Lin, F.-J., Lee, C. T., Demayo, F. J., Tsai, M.-J. and Tsai, S. Y. (2005). Suppression of Notch signalling by the COUP-TFII transcription factor regulates vein identity. *Nature* **435**, 98-104. doi:10.1038/nature03511

Zhang, H., Ge, S., He, K., Zhao, X., Wu, Y., Shao, Y. and Wu, X. (2019). FoxO1 inhibits autophagosome-lysosome fusion leading to endothelial autophagic-apoptosis in diabetes. *Cardiovasc. Res.* **115**, 2008-2020. doi:10.1093/cvr/cvz014

Zhao, Y., Yang, J., Liao, W., Liu, X., Zhang, H., Wang, S., Wang, D., Feng, J., Yu, L. and Zhu, W.-G. (2010). Cytosolic FoxO1 is essential for the induction of autophagy and tumour suppressor activity. *Nat. Cell Biol.* **12**, 665-675. doi:10.1038/ncb2069

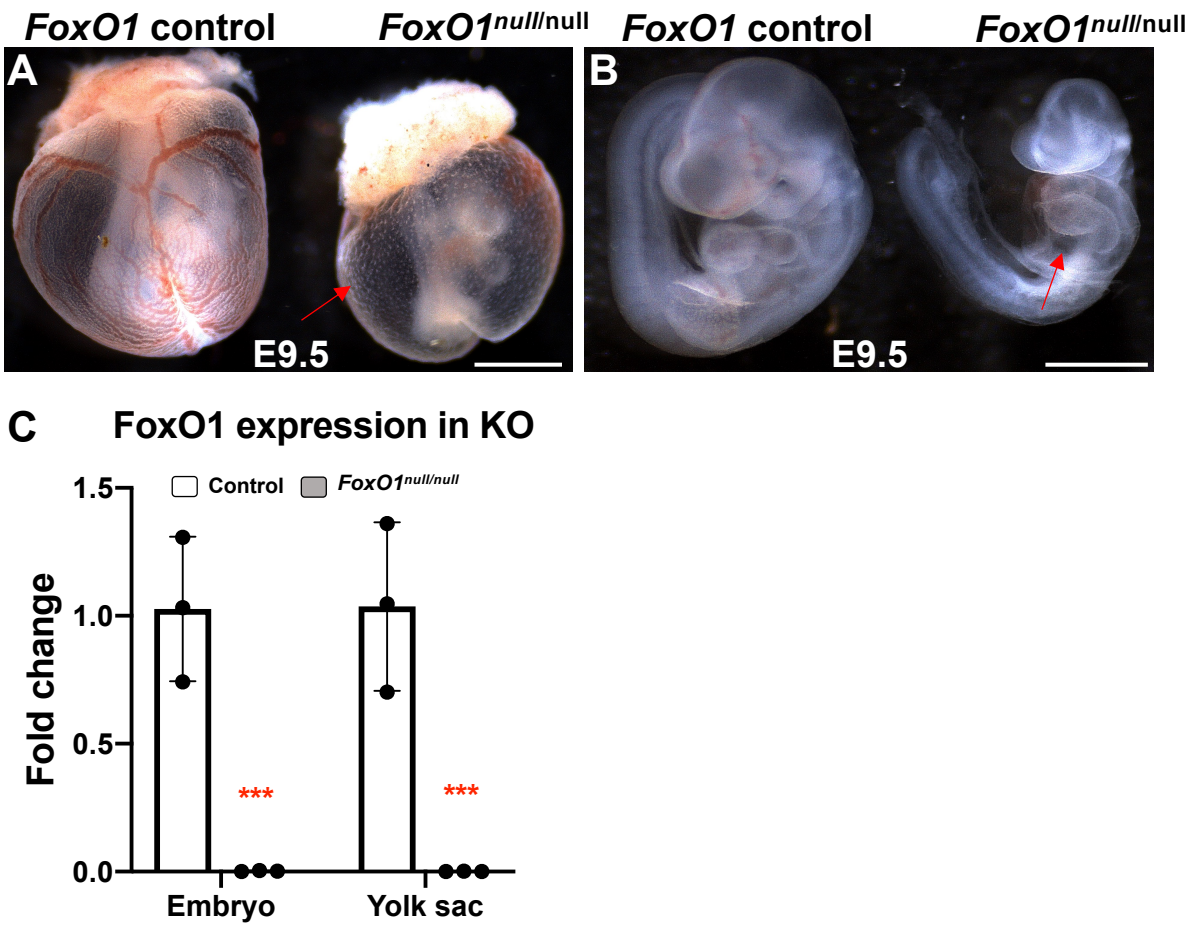

Fig. S1. *FoxO1*^{null} embryos show vascular remodeling defects. (A and B) Bright field images of E9.5 littermate control and *FoxO1*^{null} embryos in and out of the YS. (C) qRT-PCR for FoxO1 expression in control and *FoxO1*^{null} YSs.

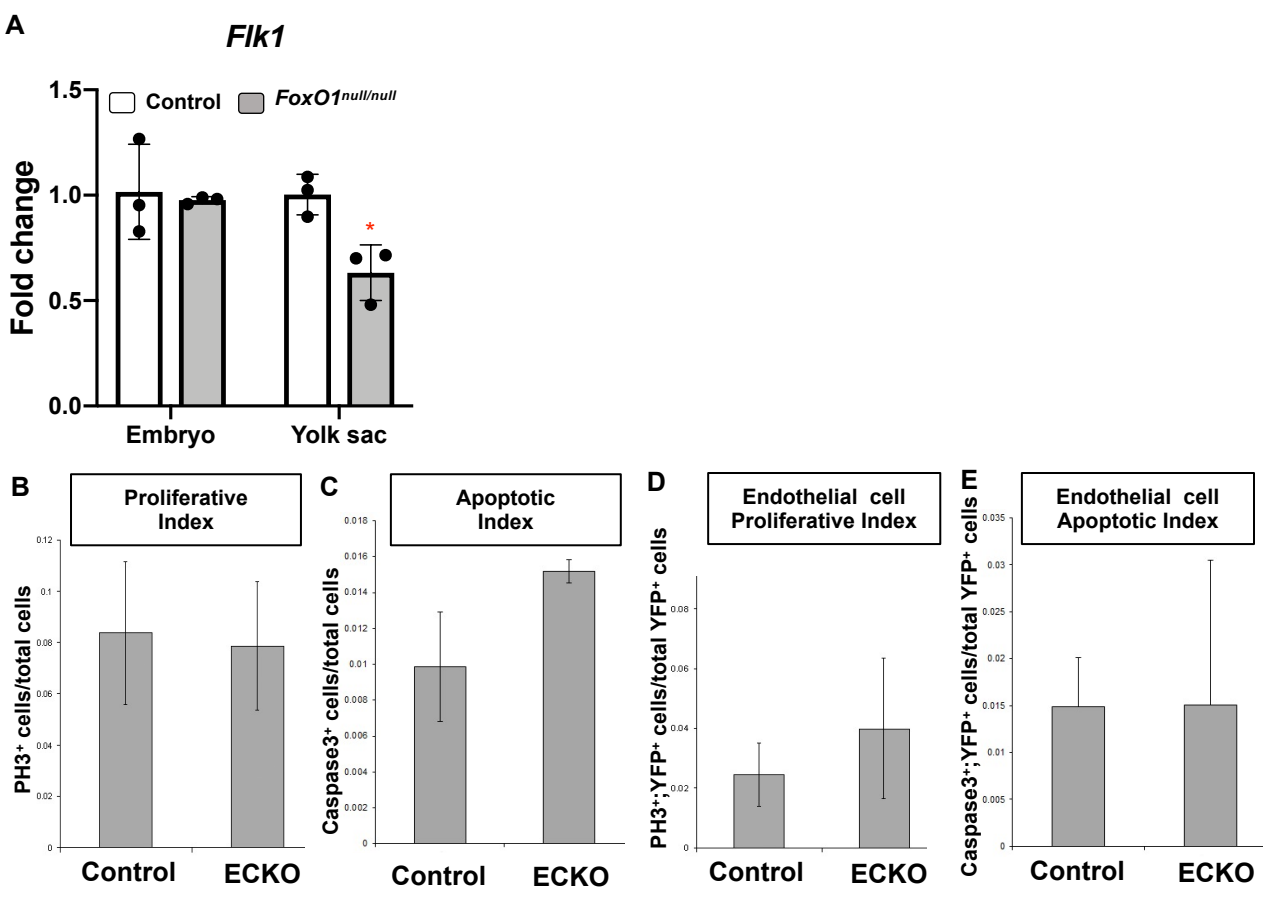

Fig. S2. (A) Flk1 expression in littermate control and *FoxO1*^{null} embryos and YSs by qRT-PCR. (B and C) Quantification of proliferation and apoptosis in littermate control and *FoxO1*^{ECKO} YSs. (D and E) Quantification of proliferation and apoptosis in littermate control and *FoxO1*^{ECKO} YS YFP+ ECs.

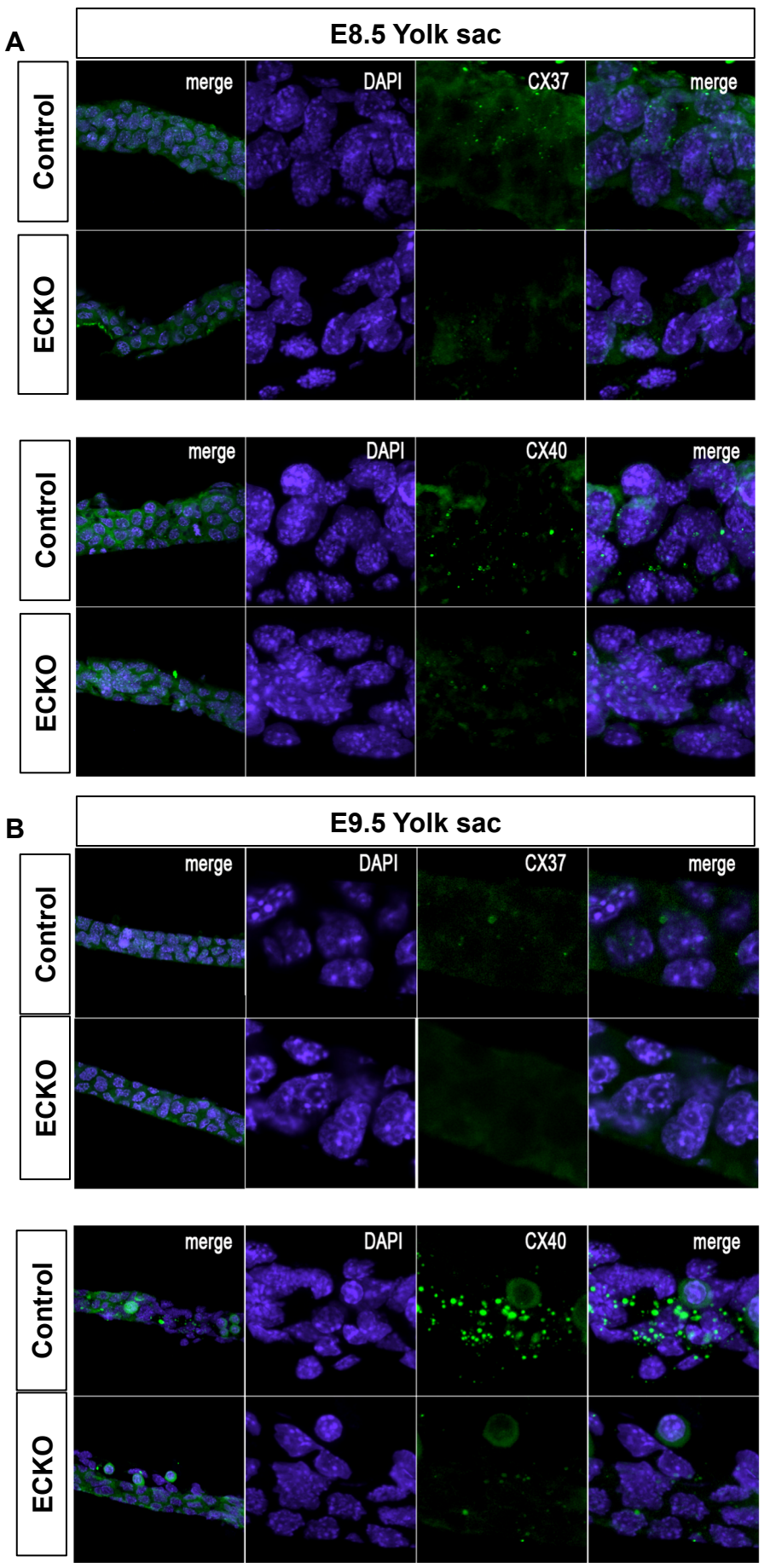

• **Fig. S3.** Co-immuno labeling of CX37, CX40and DAPI in control and *FoxO1*^{ECKO} YSs at E8.25 (A) and E9.5 (B).

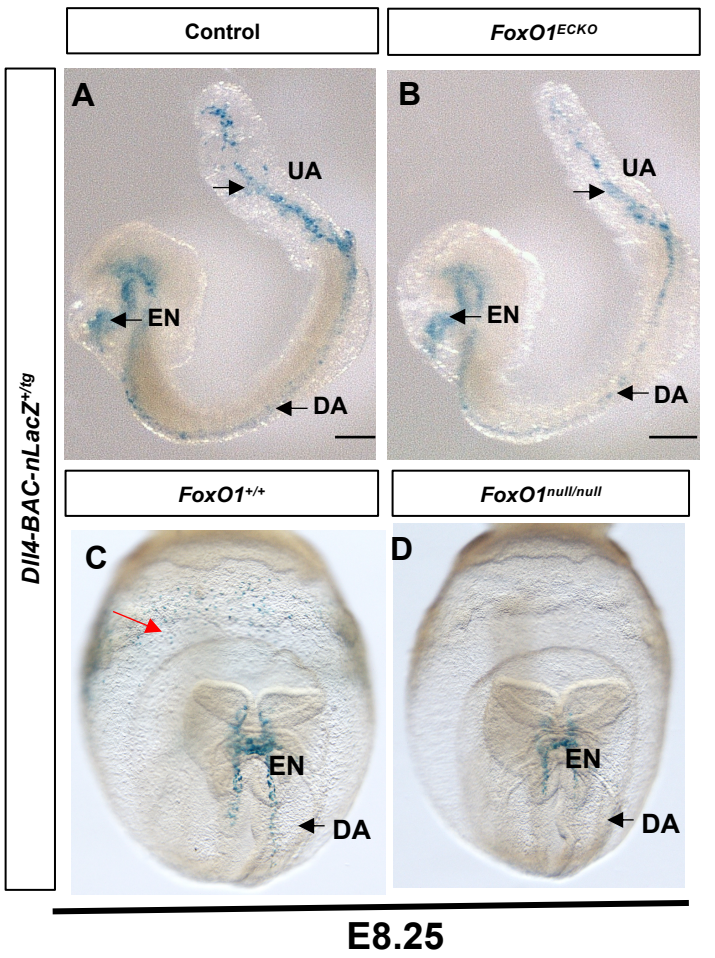

• **Fig. S4.** (A and B) *nlacZ* reporter activity in E8.25 littermate control and *FoxO1*^{ECKO} embryos dissected out of the yolk sac. (C and D) Anterior views of *nlacZ* reporter activity in E8.25 littermate control and *FoxO1*^{null} embryos. UA = umbilical artery, EN = endocardium, DA = dorsal aorta.

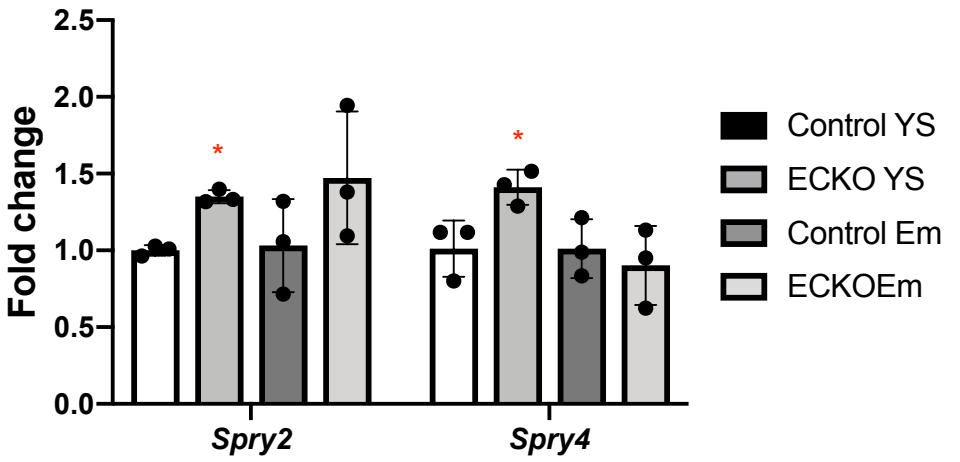

- **Fig. S5.** qRT-PCR for Sprouty2/4 in littermate control and *FoxO1*^{ECKO} YSs and embryos. Bars in graph are means± standard deviation.

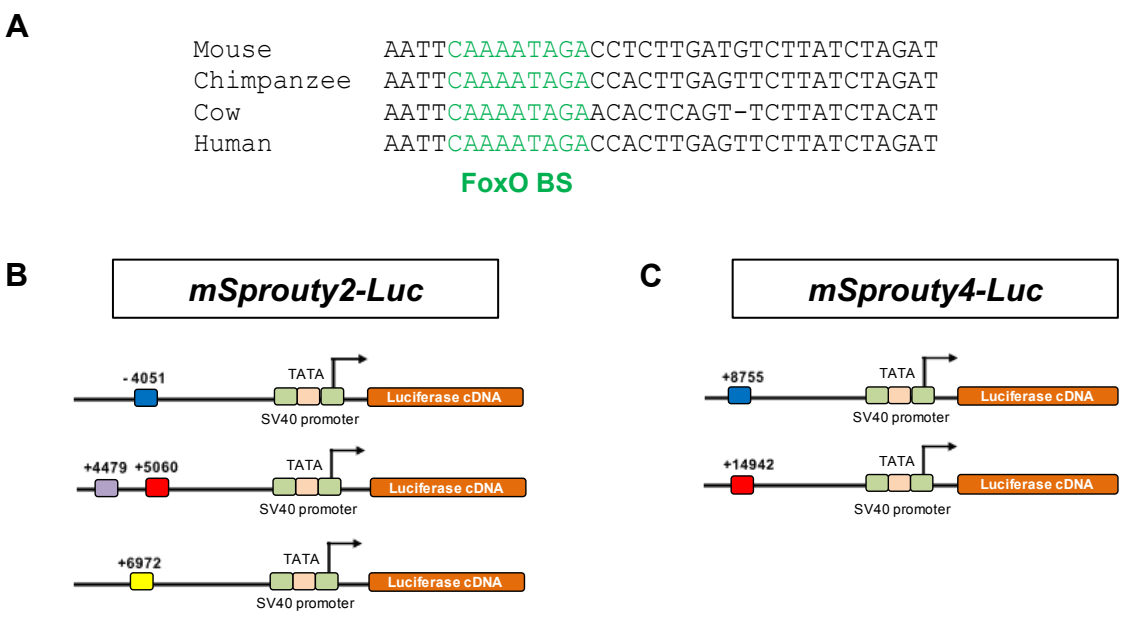

- **Fig. S6.** (A) FOXO1 conserved binding site in Mouse, Chimpanzee, Cow, and Human. (B and C) Luciferase constructs containing FOXO1 binding sites for *Sprouty2* and *Sprouty4*.

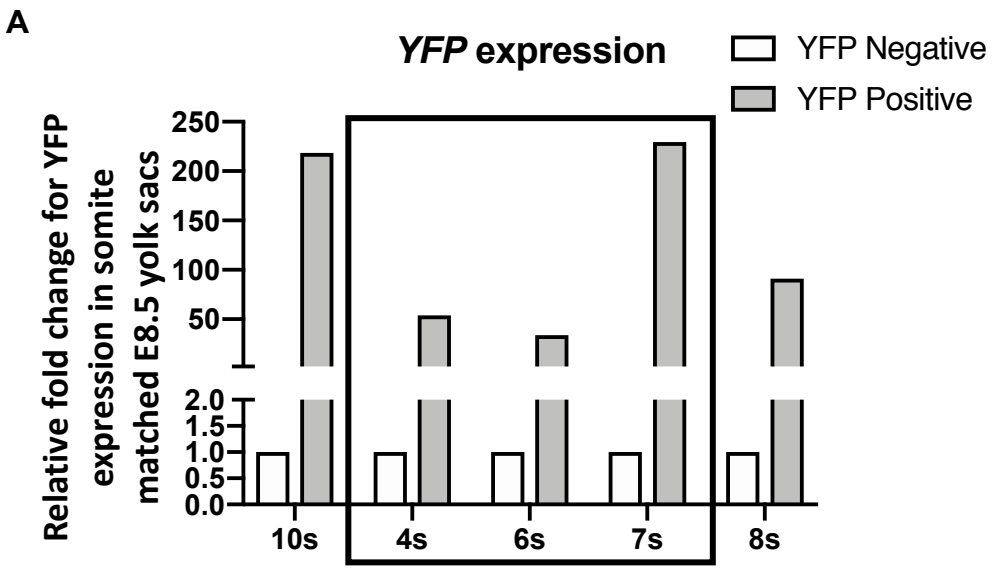

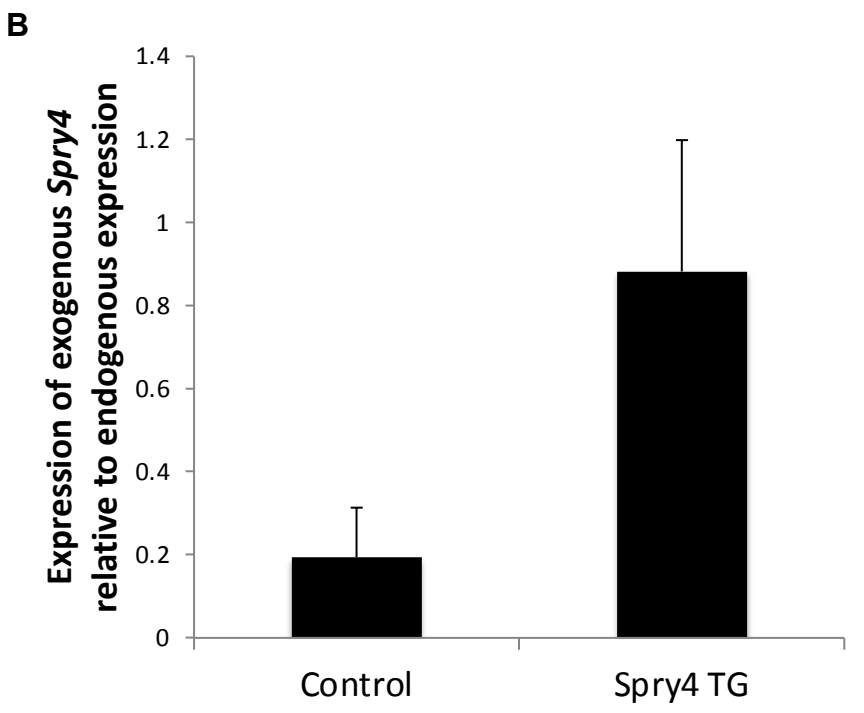

- **Fig. S7.** (A) qRT-PCR for *YFP* expression in somite matched non-trangenic (control) and transgenic embryos. Black box indicates samples that fall withing E8.25 somite stage and used for further gene analysis.
  (B) qRT-PCR for relative expression of exogenous *Sprouty4* to endogenous *Sprouty4* for all *YFP*+ transgenic embryos and somite matched controls. Bars in graph are means ± standard deviation.

Table S1. Primer sequences used for genotyping, ChIP-qPCR, and cloning

Gene/allele	Primer sequences (5'-3')	Purpose
ChIP *mSprouty2* (-4051)	TTCCAGTCCTCCAAGCAATCTAG AGTGCCTCCAGGAAGGGAAT	ChIP-qPCR
ChIP *mSprouty2* (4479)	AATTAGCAAATGGCTCCCGG TTTGTGACTGTGCCATGAAGC	ChIP-qPCR
ChIP *mSprouty2* (5060)	TAGGGCGACTCAGTGGCTATC GACCGGAGTCAAAGGACCTTC	ChIP-qPCR
ChIP *mSprouty2* (6972)	CATTTGTGTGTTTTGGGGAGAGAT CGGCAGTTGGGTTGGAATTA	ChIP-qPCR
ChIP *mSprouty4* (8755)	GATCTCCATCCGAATTCCAAATG CTTGGTTCGGCAAAGGCGAGAAAC	ChIP-qPCR
ChIP *mSprouty4* (14942)	CCACCACAAAAGTTACCACAGAAG GATATCTTCTAGATCAGTAC	ChIP-qPCR
ChIP negative control	GAAACCCGAATCTACATTCCGTTCC CTGGATTAACCCGATTATACACC	ChIP-qPCR
Luc *mSprouty2* (-4051)	GTGTACACAGGTATACTCTAGTCACCAACCC GGGACTCGATGTTGCAATGAGATACTCAACTC	PCR cloning
Luc m *Sprouty2* (4479/5060)	GATCTGTGACAAGCAGTGCCTCTGCTCAG GCCACAAGGTGACTAATGTTGTCAAGATGG	PCR cloning
Luc *mSprouty2* (6972)	CATTCAGACCTAGCACTGTGATTCATGC CAGTGTTCAGCCAAACCAGGTAGGCCTTGA	PCR cloning
Luc *mSprouty4* (8755)	CAGCGGTTCACTTGAAGCTGCCTTGACAAG CTCTGCCTCCCAACTGCTGGGATTAAAG	PCR cloning
Luc *mSprouty4* (14942)	CTGTAGCTGTTTCTGACTTCTTGGCTAGC GGCTGAAGACTCATTGTAGAATGGGTCATG	PCR cloning
Endogenous *mSpry4 cDNA*	GAAGCCTGTCCCTTGGTGCAGTTCAG CTGGTCAATGGGTAAGATGGTGAGTG	qRT-PCR
Exogenous *mSpry4 cDNA*	GCGAGGTGCAGGAATTCGTTAAGCTCTCCC CTGGTCAATGGGTAAGATGGTGAGTG	qRT-PCR

* pGL3-Promoter

Table S2. Taqman assays for Gene expression analysis

FoxO1	Mm00490672_m1	*Hey1*	Mm00468865_m1
FoxO3a	Mm01185722_m1	*Hey2*	Mm00468865_m1
FoxO4	Mm00840140_g1	*Jagged 1*	Mm00496902_m1
Flk1 (Kdr)	Mm00840140_g1	*Nrp1*	Mm00435379_m1
PECAM1	Mm01242584_m1	*Nrp2*	Mm00803099_m1
Tie2 (Tek)	Mm01242584_m1	*CoupTFII*	Mm00772789_m1
Flt1	Mm00438980_m1	*EphB4*	Mm01201157_m1
Connexin 43	Mm00438980_m1	*AFP*	Mm00431715_m1
eNOS	Mm00435217_m1	*ADM*	Mm00437438_g1
Connexin 37	Mm00433610_s1	*BMPER*	Mm01175806_m1
EphrinB2	Mm01215897_m1	*Sprouty2*	Mm00442344_m1
Notch1	Mm00435249_m1	*Sprouty4*	Mm00442345_m1
Dll4	Mm00444619_m1		